Supporting Information for

Protein Spherical Nucleic Acids for Live-Cell Chemical Analysis

Devleena Samanta,[‡,∥,§] Sasha B. Ebrahimi,[†,∥,§] Caroline D. Kusmierz, [‡,∥] Ho Fung Cheng,[‡,∥] and Chad A. Mirkin[*,‡,∥]

[†]Department of Chemical and Biological Engineering, [‡]Department of Chemistry, [∥]International Institute for Nanotechnology, Northwestern University, Evanston, Illinois 60208, United States

[§]These authors contributed equally

Contents

1. Materials and methods

1.1. Oligonucleotide design, synthesis, purification, and characterization

1.1.1. Design

We used 3 types of spherical nucleic acid (SNA)-based constructs in this study. They are

(i) Gold NanoFlares (NFs)
   a. With a pH-sensitive i-motif sequence as the recognition strand
   b. With a pH-insensitive control sequence as the recognition strand

(ii) β-galactosidase (β-gal) SNAs
   a. With a pH-sensitive i-motif sequence as the "FIT-aptamer". This construct is referred to as ProTOn
   b. With a pH-insensitive control sequence

(iii) Glucose oxidase SNAs (GOx-SNAs)

The DNA sequences used in designing the SNAs are provided in Table S1. D denotes the location of the forced intercalation dye thiazole orange (TO) in the sequence. Note that the 7th T from the 5' end in the design of GOx-SNAs is modified with an amino group (amino-modifier C2 dT).

Table S1. Oligonucleotide sequences used in this study

Abbreviation	Sequence (from 5' end to 3' end)
Gold NF i-motif recognition	CCC TAA CCC TAA CCC TAA CCC Cy5 T_{15}-SH
Gold NF control recognition	TTT CTA TCG CGT ACA ATC TGC Cy5 T_{15}-SH
Gold NF i-motif flare	Cy3-A_6 AGG GTT AGG GTT A
Gold NF control flare	Cy3-A_6 AGC AGA TTG TAC G
ProSNA i-motif	DBCO TEG- T_{15} C_4 TAA CDCC TAA C_4 TAA CTCC
ProSNA control	DBCO TEG- T_{15} T_4 TTT TDTT TTT T_4 TTT TTTT
GOx DNA	DBCO TEG- T_{13}

Cy3 denotes cyanine-3. Cy5 denotes cyanine-5. DBCO-TEG denotes 10-(6-oxo-6-(dibenzo[b,f]azacyclooct-4-yn-1-yl)-capramido-N-ethyl)-O-triethyleneglycol-1-[(2-cyanoethyl)-(N,N-diisopropyl)]-phosphoramidite.

1.1.2. Synthesis, purification, and characterization

All reagents for DNA synthesis were purchased from Glen Research. Oligonucleotides were synthesized using solid-phase phosphoramidite coupling chemistry. Universal or thiolated controlled pore glass (CPG) beads were used as the solid support. Synthesis was performed either using a MerMade12 (MM12, BioAutomation Inc., Plano, Texas, USA) or an ABI 394 instrument at 5 or 10 µmol scales. The oligonucleotides were then cleaved from the CPG beads using standard deprotection techniques (4 h at 55 ºC or 16 h at room temperature using 2 mL of 30% ammonium hydroxide). An Organomation® Multivap® Nitrogen Evaporator was then used to evaporate off the ammonia. The remaining solution was adjusted to 2 mL in volume using nanopure water and filtered through a 0.2 µM syringe filter to remove the CPG beads. The filtrate was subjected to reverse phase high-performance liquid chromatography (RP-HPLC, Varian ProStar 210, Agilent Technologies Inc., Palo Alto, CA, USA) to isolate the product. A C4 or C18 column and a gradient of 0 to 75% B over 45 min (A = triethylammonium acetate buffer, B = acetonitrile) were used. The collected fractions for sequences terminating in a 4,4'-dimethoxytrityl (DMTr) group were lyophilized and re-dissolved in 20% acetic acid for 1 h for detritylation. The cleaved DMTr group was removed by ethyl acetate extraction (3 times). The remaining acidic solution was lyophilized and re-dissolved in water. Sequences not terminating in a DMTr group did not require treatment with acetic acid. Matrix-assisted laser desorption ionization time-of-flight mass spectrometry (MALDI-TOF MS) was used to identify the product. The concentration (c) of the final product was determined using UV-vis spectroscopy. Specifically, $c = A/\varepsilon$ where A is the absorbance measured and ε is the extinction coefficient of the oligonucleotide at 260 nm obtained from the IDT Oligo Analyzer Tool.

1.2. Synthesis and characterization of thiazole orange (TO)

1.2.1. General methods

All of the chemicals, reagents, and solvents were purchased as reagent grade from Sigma-Aldrich and used as received unless otherwise stated. Glassware and stir bars were oven-dried at 180 ℃ prior to use. Flash chromatography was performed with SiO_2 (230–400 mesh ASTM, 0.040–0.063 mm; Fluka). Deuterated solvents were purchased from Cambridge Isotope Laboratories and used as received. ^1H and ^{13}C NMR spectra were recorded on a Bruker Avance 400 MHz NMR spectrometer at 298 K, and chemical shifts (δ) are given in parts per million. ^1H NMR spectra were referenced to residual proton resonances in the deuterated solvents (methanol-d_4 = δ 3.31), while absolute referencing was applied for heteronuclear NMR spectra (Ξ_C = 25.145020). N-carboxylmethyl-4-methquinolinium bromide was synthesized following literature procedures.[1]

1.2.2. Synthesis of thiazole orange derivative

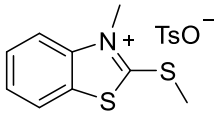

3-Methyl-2-(methylthio)-benzothiazolium tosylate was synthesized as described previously with slight modifications.[1] Solid 2-methylthiobenzothiazole (4.12 g, 22.7 mmol, 1 equiv) was added to neat methyl p-toluenesulfonate (4.66 g, 25 mmol, 1.1 equiv) in an oven-dried round bottom flask and heated to reflux at 130 °C for 1 h. The reaction mixture was cooled to 70 °C, and acetone was added till creamy precipitates formed. The reaction was then refluxed at 70 °C. After 30 min, the mixture was cooled to room temperature, filtered, and washed with acetone. The creamy precipitates collected were dried in vacuo to yield the product (8.11 g, 22.1 mmol, isolated yield = 97 %). ^1H NMR (400 MHz, methanol-d_4) δ 8.20 (ddd, J = 8.2, 1.3, 0.7 Hz, 1H), 8.05 (dt, J = 8.6, 0.8 Hz, 1H), 7.82 (ddd, J = 8.5, 7.3, 1.2 Hz, 1H), 7.71 (ddd, J = 8.3, 7.3, 1.0 Hz, 1H), 7.69 – 7.61 (m, 2H), 7.22 – 7.14 (m, 2H), 4.12 (s, 3H), 3.10 (s, 3H), 2.33 (s, 3H). ^{13}C NMR (101 MHz, MeOD) δ 181.12, 141.97, 141.63, 139.45, 128.62, 127.78, 127.65, 126.41, 124.80, 122.53, 114.37, 34.77, 19.20, 16.42.

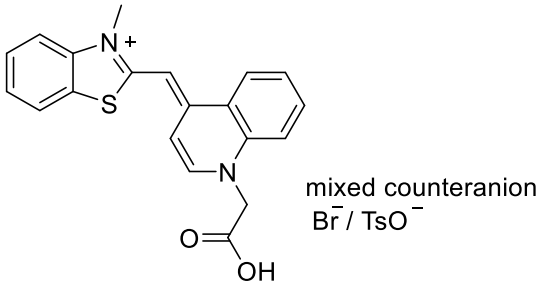

Carboxymethylated thiazole orange was synthesized as described previously with slight modifications.[1] N-carboxylmethyl-4-methquinolinium bromide (1.52 g, 5.39 mmol, 1.25 equiv) and 3-methyl-2-(methylthio)-benzothiazolium tosylate (1.58 g, 4.31 mmol, 1 equiv) were dissolved in dichloromethane. Triethylamine (1.5 mL, 10.8 mmol, 2.5 equiv) was then added. The reaction mixture, which turned dark red immediately, was stirred in the dark at room temperature for 16 h. The reaction mixture was dried on a rotary evaporator to give a red residue, which was dissolved in 325 mL of boiling methanol. 815 mL of water was then added to the red solution, which was stored at 4 °C for 3 days during crystallization. The red precipitate formed was collected by filtration, washed with a small amount of cold water, and dried in vacuo to give a red powder (1.64 g, 3.83 mmol, 89 % isolated yield). Note that the product gradually decomposes in solution if it is exposed to light. ^{1}H NMR (400 MHz, methanol-*d*$_4$) δ 8.66 – 8.60 (m, 1H), 8.34 (d, J = 7.2 Hz, 1H), 7.96 – 7.86 (m, 2H), 7.75 – 7.56 (m, 4H), 7.49 (dd, J = 7.2, 2.3 Hz, 1H), 7.46 – 7.37 (m, 1H), 6.93 (s, 1H), 5.17 (s, 2H), 4.00 (s, 3H).

1.2.3. NMR spectra

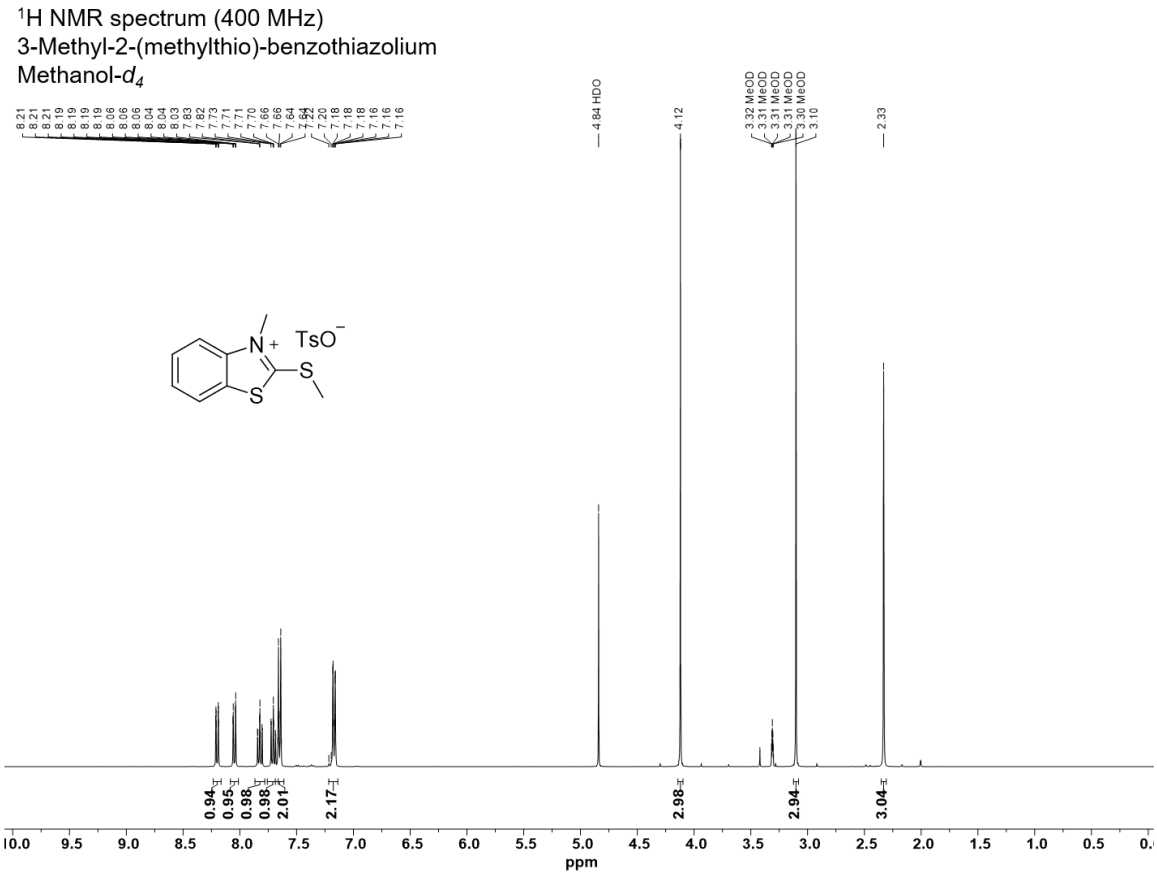

Figure S1. ^{1}H NMR (400 MHz, methanol-d_4, 298 K) spectrum of 3-methyl-2-(methylthio)-benzothiazolium tosylate.

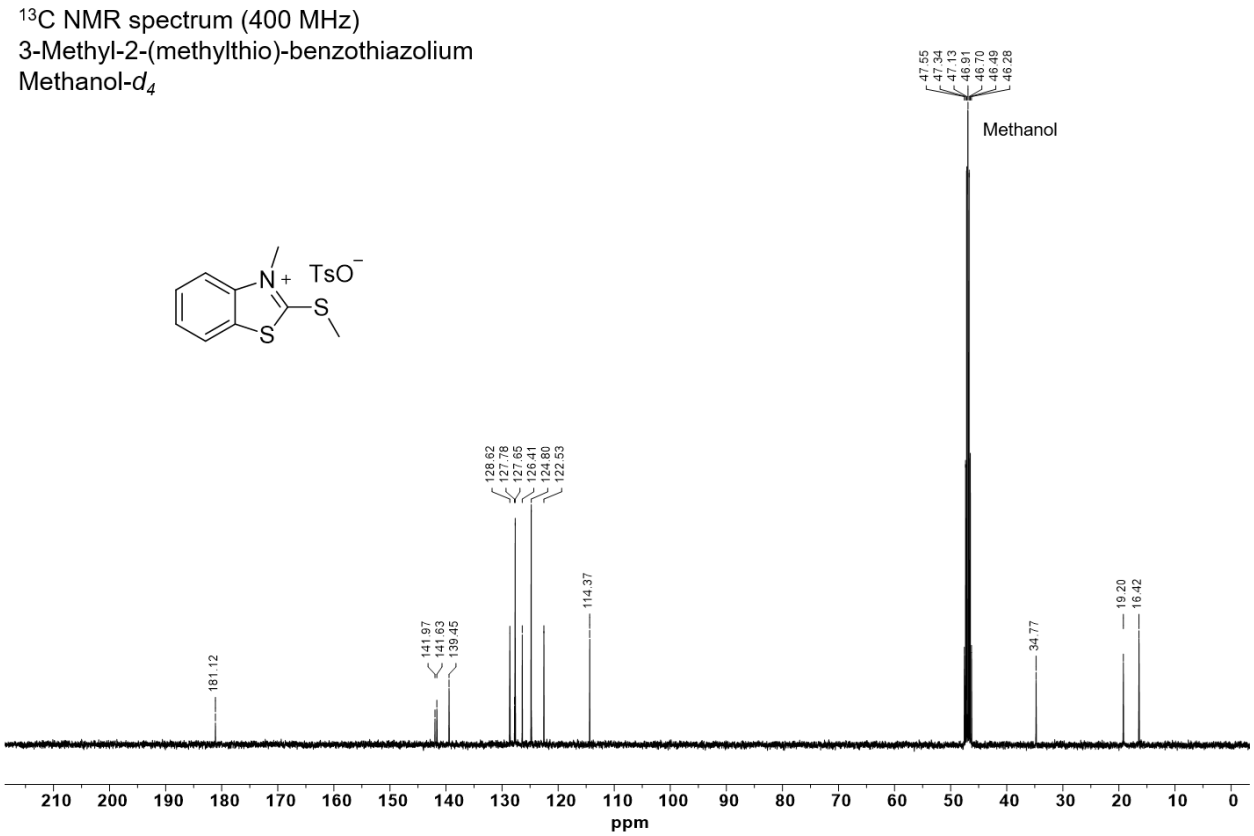

Figure S2. ^{13}C NMR (101 MHz, methanol-d_4, 298 K) spectrum of 3-methyl-2-(methylthio)-benzothiazolium tosylate.

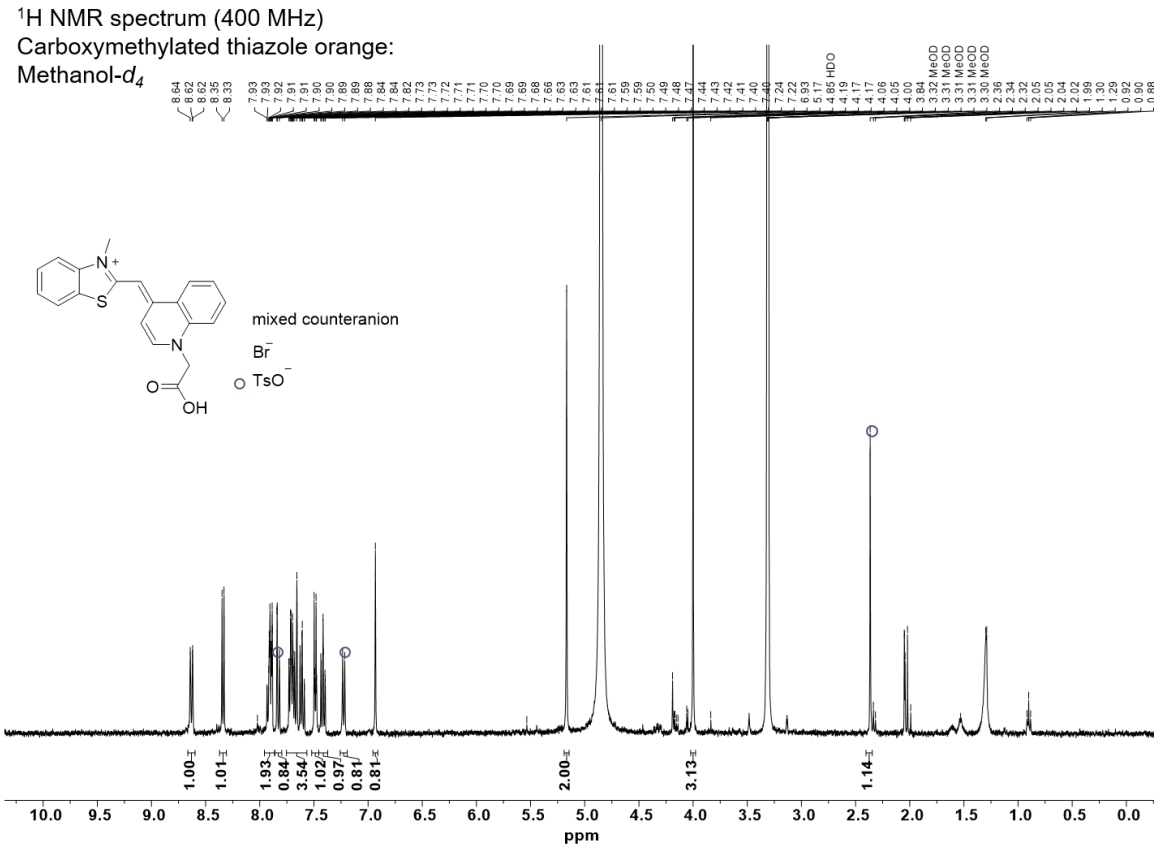

Figure S3. ^{1}H NMR (400 MHz, methanol-d_4, 298 K) spectrum of carboxymethylated thiazole orange.

1.3. Coupling of TO to oligonucleotide probes

Thiazole orange was conjugated to DNA sequences composed of an amino-modifier (N-trifluoroacetyl serinol phosphoramidite) according to a previously reported protocol.[2] In a typical reaction, thiazole orange (5 µmol), pyridinium para-toluene sulfonate (5 µmol), N-hydroxysuccinimide (25 µmol), and 1-Ethyl-3-(3- dimethylaminopropyl) carbodiimide (50 µmol) were dissolved in 250 µL dimethylformamide and shaken for 10 min at 30 °C. After 10 min, 100 nmol of amino-modified DNA in 250 µL of 0.1 M $NaHCO_3$ was added to the solution and shaken at room temperature for 2 h. After 2 h, the reaction mixture was run through a NAP™-10 (GE Healthcare) column to separate away any free dye. To separate DNA sequences with and without the dye modification, RP-HPLC was then run on a C18 column (0 to 75% B, 45 min, A = triethylammonium acetate buffer, B = acetonitrile).

1.4. Synthesis, purification, and characterization of i-motif and control gold NFs

In a typical reaction, 2 mL of 13 nm gold NPs were added to a 15 mL falcon tube and supplemented with Tween 20 to a final concentration of 0.2%. 10X PBS was added to the falcon tube such that its final concentration became 1X. The mixture was vortexed for 30 s and then sonicated for 30 s.

In a separate tube, recognition and flare strands were mixed in a 1:1 molar ratio and adjusted to 50 µM concentration in 1X duplexing buffer (30 mM HEPES, 100 mM KOAc, 2 mM MgOAc). This mixture was heated at 95 °C for 5 min and then allowed to cool to room temperature. The duplex was then added to the AuNP mixture at 300 equiv. duplex per AuNP. The subsequent mixture was allowed to incubate for 2 h, at which point 5 M NaCl was added to make the NaCl concentration 350 mM. After 1 h of further incubation, more 5 M NaCl was added to make the final NaCl concentration 500 mM. The mixture was then shaken for 48 h. After 48 h, the gold NFs were purified using 5 rounds of centrifugation (15000 rcf, 10 min) through successive pelleting and resuspension steps in 1X PBS.

The concentration of the gold NFs was determined via UV-vis spectroscopy using an extinction coefficient of 2.7×10^8 $M^{-1}cm^{-1}$ for 13 nm gold nanoparticles.[3] Next, the number of DNA strands per particle was determined. 40 µL of 50 nM gold NFs was added to 140 uL 8 M urea. 180 µL of 40 mM KCN was added to this mixture. Over the next 5-10 min, the gold nanoparticles were etched completely by KCN and this process could be followed visually as the wine-red color of

the nanoparticles disappeared. The solution was heated to 60 ºC for 10 min. The fluorescence of the resultant solution was measured using a plate reader both in the Cy3 (excitation: 554 nm, emission 600 nm) and Cy5 (excitation: 647 nm, emission: 700 nm) channels. The concentration of DNA could be calculated from a calibration curve of the Cy3- and Cy5-labeled recognition and flare strands in the same solvent mixture. All fluorescence measurements were performed in triplicate. The ratio of the concentration of DNA to that of the nanoparticles yielded the number of strands per particle. On average, each gold nanoparticle had ~40 duplexes (one flare strand for every recognition strand).

1.5. Synthesis of ProSNAs

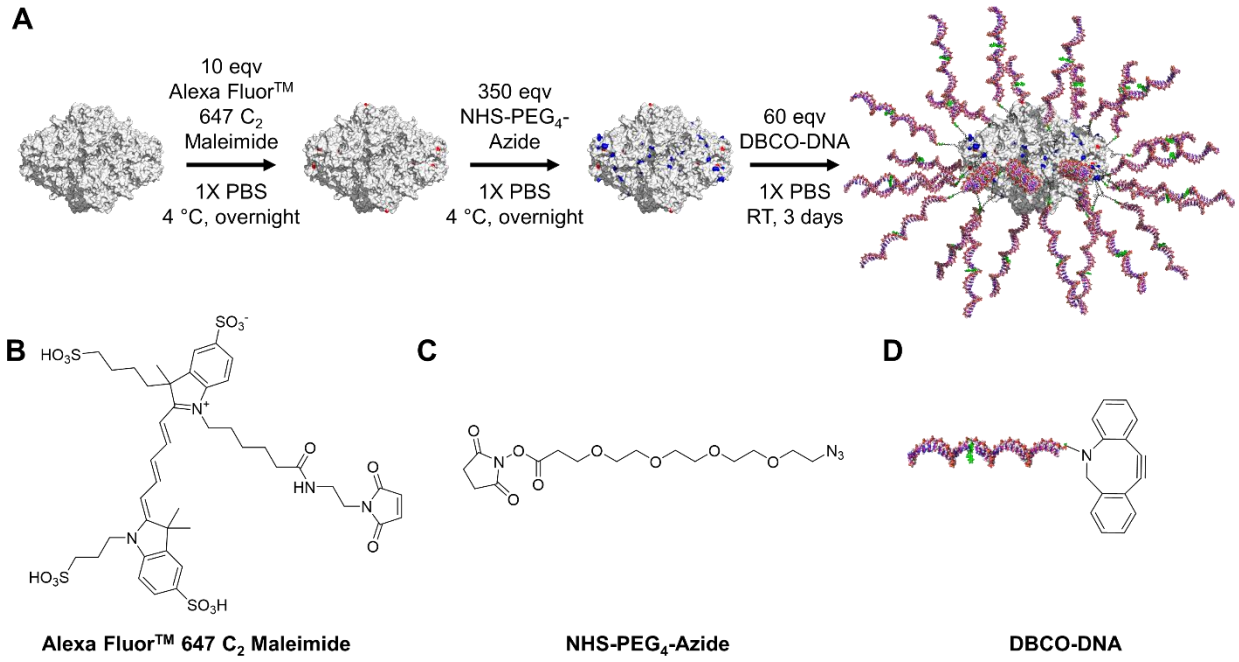

Figure S4. General scheme for the synthesis of ProSNAs. (A) Surface cysteine groups are first modified with Alexa Fluor™ 647 C_2 maleimide (highlighted in red). Then, NHS-PEG_4-azides are conjugated to the surface-accessible lysine residues (highlighted in blue). Finally, DBCO-terminated DNA is attached to the azide-modified proteins through copper-free click chemistry. Structures of (B) Alexa Fluor™ 647 C_2 maleimide, (C) NHS-PEG_4-azide, and (D) DBCO-terminated DNA. It should be noted that the scheme shown here was used for the synthesis of β-gal ProSNAs. For the synthesis of GOx-SNAs, the procedure was slightly modified. In this case, Alexa Fluor™ 647 NHS ester was conjugated through lysine residues due to the lack of surface cysteines.

1.5.1. Synthesis, purification, and characterization of i-motif and control ProSNAs

β-galactosidase (β-gal) ProSNAs were synthesized and characterized following previously reported procedures.[4,5] Lyophilized β-gal from an E. coli overproducer (Roche) was centrifuged and resuspended in 1X PBS three times using a 100 kDa MWCO Amicon® filter to remove storage salts. Next, a thiol-reactive Alexa Fluor™ 647 C_2 Maleimide (ThermoFisher), AF-647, was introduced at a ten-fold excess, and the reaction was allowed to proceed overnight at 4 °C in 1X PBS with shaking. Multiple washing cycles were conducted in a 100 kDa MWCO Amicon® filter to remove the unreacted dye, resuspending β-Gal-AF-647 in 1X PBS after each centrifuge. Wash cycles were stopped once the filtrate did not have a detectable absorbance signal at ~653 nm, as monitored by a Cary-500 UV-vis spectrophotometer. A 350-fold excess of NHS-PEG_4-Azide (ThermoFisher) was added to β-Gal-AF-647 and incubated overnight at 4 °C in 1X PBS with shaking. Unreacted linker was removed by ten wash cycles using a 100 kDa MWCO Amicon® filter, and resuspending the β-Gal-AF-647-azide in 1X PBS after each centrifugation. The number of AF-647 modifications made to the protein were calculated based on absorbance spectra collected on a Cary-500 UV-vis spectrophotometer and their respective extinction coefficients ($\varepsilon_{\beta\text{-gal}}$ = 1,142,000 $M^{-1}cm^{-1}$ at 280 nm and 596,268 $M^{-1}cm^{-1}$ at 260 nm; $\varepsilon_{\text{AF-647}}$ = 270,000 at 650 nm). The number of PEG_4-azide linker modifications was assessed by MALDI-TOF MS using sinapinic acid (ThermoFisher) as a matrix in a Bruker AutoFlex-III. Each linker addition leads to an increase of 275 m/z. In a typical reaction, 60 molar equivalents (DNA:protein) of DBCO-modified DNA was added to a 1.5 mL Eppendorf tube and dried on a Centrivap. Protein (1X PBS, concentration ~6 μM β-gal) was then added to this DNA and shaken for 3 days (60 eq DNA:protein). After 3 days, the ProSNAs were purified through ~15-20 washes (1X PBS) using a 100 kDa Amicon filter. The number of DNA strands per protein was calculated based on UV-vis spectroscopy ($\varepsilon_{\text{i-motif DNA}}$ = 337,600 $M^{-1}cm^{-1}$ at 260 nm and $\varepsilon_{\text{control DNA}}$ = 315,400 $M^{-1}cm^{-1}$ at 260 nm). Because the DNA's max absorbance (260 nm) overlaps with the protein's max absorbance (280 nm), the AF-647 UV-vis trace was used to back-calculate the protein's concentration. There were ~6.8 AF-647 dyes per protein. ~30 DNA strands were attached per i-motif ProSNA (ProTOn) and ~40 DNA strands per control ProSNA.

1.5.2. Design, synthesis, purification, and characterization of GOx-SNAs

Due to the absence of chemically accessible cysteine residues on the surface of glucose oxidase (GOx), both AF-647 and DNA were conjugated to the surface through lysine residues. The relative

ratios of the two modifications were controlled by controlling the molar equivalents and the conjugation reaction time. On average, each protein contained ~2 AF-647 dyes and ~28 DNA strands. A simple DBCO-labeled T_{13} sequence was used as the DNA shell to enable probe uptake and as in the case of β-gal, the AF-647 dyes allow for monitoring of probe uptake.

Glucose oxidase protein (Millipore-Sigma G7141) was first dissolved in 0.1 M $NaHCO_3$ at 10 mg/mL. Alexa Fluor™ 647 NHS Ester (Thermo-Fisher A37573) was dissolved at a concentration 10 mg/mL in DMF. This dye solution was added dropwise to the protein solution while vortexing in 13-fold molar excess. After shaking the mixture for 1 h at 1400 rpm, the unfunctionalized AF-647 was separated from the protein using a 30 kDa Amicon filter (13,000 rcf at 4 ºC) and washing 10 times using 0.1 M $NaHCO_3$.

The protein was then labeled with PEG-azide to allow subsequent functionalization to DBCO-modified DNA. 300 µL of 50 µM protein in PBS was reacted with 18 µL NHS-PEG_4-Azide for 1.75 h. The mixture was then purified using a 30 kDa Amicon filter by washing with 1X PBS (10 washes, 13,000 rcf at 4 °C).

In a typical DNA functionalization reaction, 300 molar equivalents (DNA:protein) of DBCO-modified DNA was added to a 1.5 mL Eppendorf tube and dried on a Centrivap. Protein (1X PBS, concentration ~10 µM) was then added to this DNA and shaken for 3 days (300 eq DNA:protein). After 3 days, GOx-SNAs were purified through ~15-20 washes (1X PBS) using a 100 kDa Amicon filter.

The number of dyes and DNA strands per protein was calculated via UV-vis spectroscopy using the extinction coefficient of the DNA (ε_{DNA} = 113,900 $M^{-1}cm^{-1}$), protein (ε_{GOx} = 267,200 $M^{-1}cm^{-1}$), and the dye ($\varepsilon_{AF\text{-}647}$ = 270,000 $M^{-1}cm^{-1}$).

1.6. Fluorescence experiments

All experiments were done in triplicate unless otherwise stated.

1.6.1. Experiments with i-motif and control gold NFs

1.6.1.1. Fluorescence melt to determine duplex melting temperature

The melting temperature of the flare/recognition strand duplex was determined by fluorescence melt experiments. This was done to ensure that the i-motif recognition/flare and control recognition/flare have comparable melting temperatures. ~3 nM by gold i-motif or control NFs were added to pH 7.5 clamping buffer (Thermo-Fisher P35379). The temperature of a BioTek Cytation 5 fluorescence plate reader was set to *x* °C (where *x* = 28, 29, 31, 33, 35, 37, 39, 41, 43, 45, 47, 49, 51, 53, 55, 57, 59, 61, 63, 65) and samples were shaken for 5 min. After 5 min, a fluorescence reading was taken, acquiring a fluorescence reading at each temperature (excitation: 554 nm, emission: 600 nm for the Cy3 dye; excitation: 647 nm, emission: 700 nm for the Cy5 dye).

1.6.1.2. pH sensitivity of i-motif gold NFs in buffer

i-motif or control NFs were incubated in clamping buffer of varying pH to assess the response of the constructs to pH. The pH of buffer was adjusted using NaOH. 1.7 nM by gold i-motif or control NF was added to buffer of pH 4.5 5.0, 5.5, 6.0, 6.5, 7.0, and 7.5 and incubated for 30 min at 37 °C. A BioTek Cytation 5 fluorescence plate reader (excitation 554 nm, emission 600 nm for the Cy3 dye, excitation 647 nm, emission 690 nm for the Cy5 dye) was used to measure the fluorescence at each pH.

1.6.1.3. Fluorescence response of gold NFs in presence of nuclease in buffer

In triplicate, 2 nM gold NFs (by gold) was added to 100 µL 1X DNAse buffer and allowed to incubate at 37 °C for 30 min. After 30 min, 10 µL of 0.2 U/µL DNAse I (Themo-Fisher AM2224) was added to each well (10 µL of water was added to wells not treated with DNAse as a DNAse free control). Fluorescence was monitored on a BioTek Cytation 5 plate reader (excitation 554 nm, emission 600 nm for the Cy3 dye, excitation 647 nm, emission 690 nm for the Cy5 dye) every 1 min over the course of 15 min.

1.6.1.4. Change of fluorescence signal over time of gold NFs *in cellulo*

MDA-MB-231 cells were treated in a 24 well plate with 1 nM (by gold) control NFs in Opti-MEM (Thermo-Fisher 31985062). All cells were pulsed for 1 h and chased for either 0, 2, or 4 h in triplicate. Cells were washed with 400 µL Opti-MEM before the pulsing step and 400 µL Opti-MEM before the chasing step. After the chasing step, cells were detached from the plate using 1X

TrypLE (Thermo-Fisher 12604021) with added 4′,6-diamidino-2-phenylindole (DAPI) and then analyzed using flow cytometry (BD LSRFortessa and BD Symphony A3).

1.6.2. Experiments with i-motif and control ProSNAs

1.6.2.1. pH sensitivity of ProTOn in buffer

i-motif or control ProSNAs were incubated in clamping buffer of varying pH to assess the response of the constructs to pH. 500 nM (by DNA) of ProTOn or control ProSNA were added to buffer of pH 5.0, 5.5, 6.0, 6.5, 7.0, and 7.5 in triplicate at room temperature. A BioTek Cytation 5 fluorescence plate reader (excitation 485 nm, emission 528 nm for the thiazole orange dye, excitation 647 nm, emission 690 nm for the AF-647 dye) was used to measure the fluorescence at each pH.

1.6.2.2. Fluorescence response of ProSNAs in presence of nuclease in buffer

In triplicate, 500 nM (by DNA) of i-motif or control ProSNA was added to 100 µL 1X DNAse buffer and incubated at 37 °C for 15 min. 10 µL of 0.2 U/µL DNAse I was added to induce nuclease degradation. 10 µL of water was added to the wells not treated with DNAse I as a control. The fluorescence was monitored on a BioTek Cytation 5 plate reader (excitation 485nm, emission 528 nm for the thiazole orange dye) every 1 min over the course of 15 min.

1.6.2.3. Response of ProSNAs to proteases in buffer

For this specific study, the ProSNA used was comprised of β-gal densely functionalized with a DBCO-dT-$(sp18)_2T_{30}$ sequence (~34 DNA per protein). The native protein and the ProSNA were incubated with 250 mg/L Trypsin (Gibco) in 1X PBS at 37°C with shaking. As the degradation reaction proceeded, aliquots were removed every 10 min for a total of 70 min and loaded onto a 7.5% Mini-PROTEAN TGX precast gel (BioRad). The samples were loaded onto the gel using Laemmli sample buffer (BioRad) and the gel was run at 100V for 1.5 h in TGS running buffer. The protein bands were visualized by staining using a SimplyBlue SafeStain (Thermo Fisher).

1.6.2.4. Change of fluorescence signal over time of ProSNAs *in cellulo*

MDA-MB-231 cells were treated in a 24 well plate with 500 nM (by DNA) control ProSNAs. All cells were pulsed for 1 h and chased for either 0, 2, or 4 h in triplicate. Cells were washed with

400 µL Opti-MEM before the pulsing step and 400 µL Opti-MEM before the chasing step. After the chasing step, cells were detached from the plate using 1X TrypLE containing DAPI and then analyzed using flow cytometry.

1.6.2.5. Fluorescence response of i-motif ProSNA after clamping cellular pH

MDA-MB-231 cells were treated in a 24 well plate with 500 nM (by DNA) of ProTOn or control ProSNA. Cells were treated for 3 h, after which they were washed once with 400 µL Opti-MEM and subsequently detached using 1X TrypLE. Each well of the plate was then pipetted into separate Eppendorf tubes, after which tubes were centrifuged to pellet the cells. The supernatant was aspirated off, and cells were suspended in pH 5.5 or pH 7.5 clamping buffer for 10 min before being analyzed by flow cytometry. Control cells not treated with SNAs were also analyzed to ensure that different pH's do not alter the autofluorescence of the cells. As a control, commercially available pHrodo™ Red AM Intracellular pH Indicator (Thermo Fisher P35372) was also used to measure the fluorescence difference between cells clamped at pH 5.5 and pH 7.5. Cells were treated according to manufacturer protocol with no modification.

1.6.3. Experiments with GOx-SNAs

1.6.3.1. Fluorescence response of GOx-SNAs to glucose in buffer

Varying concentrations of glucose (in 1X PBS) were added to the wells of a 96 well plate, whereby the concentration of glucose was halved in each well through a half serial dilution (a separate set of wells were prepared that had 0 mM glucose). All wells contained 5 µM FBBBE (Cayman Chemical 14606). The plate was then allowed to incubate for 30 min at 37 °C. After 30 min, an automatic dispensing unit on a BioTek Cytation 5 fluorescence plate reader was used to add GOx-SNAs to each well at a final concentration of 20 nM by protein (a buffer only set of wells was also prepared). After addition, the BioTek Cytation 5 plate reader was used to shake the sample for 15 s, and subsequently a fluorescence reading was taken every 3 min over 2 h (excitation 460 nm, emission 530 nm for FBBBE, excitation 640 nm, emission 700 nm for the Alexa Fluor 647 dye).

A separate control experiment was done to ensure that the dye fluorescence in the absence of GOx-SNAs does not change with increasing glucose concentration. Varying concentrations of glucose (in 1X PBS) were added to the wells of a 96 well plate, whereby the concentration of glucose was halved in each well through a half serial dilution (a separate set of wells were prepared that had

0 mM glucose). All wells contained 5 μM FBBBE. The samples were incubated at 37°C for 30 min, after which a fluorescence reading was taken every 3 min over 2 h (excitation 460 nm, emission 530 nm for FBBBE).

1.6.3.2. GOx-SNAs fluorescence response to "off-target" sugars in buffer

In triplicate, 20 nM (by protein) GOx-SNAs was co-incubated with 5 μM FBBBE and one different sugar (either 5 mM glucose, sucrose, xylose, mannose, glucose 6-phosphate, fructose, maltose, lactose, or galactose) in 1X PBS. Controls for GOx-SNAs+FBBBE, FBBBE only, GOx-SNAs only, and 1X PBS only were also done. Samples were incubated at 37 °C for 30 min after which a fluorescence reading was taken on a BioTek Cytation 5 plate reader (excitation 460 nm, emission 530 nm for the FBBBE dye).

In another experiment, 10 nM (by protein) GOx-SNAs were incubated with 5 μM FBBBE and all the sugars (5 mM glucose, sucrose, xylose, mannose, glucose 6-phosphate, fructose, maltose, lactose, and galactose) in 1X PBS. Controls for GOx-SNAs+FBBBE+5 mM glucose, GOx-SNAs+FBBBE, FBBBE only, GOx-SNAs only, and 1X PBS only were also done. Samples were incubated at 37 °C for 30 min after which a fluorescence reading was taken on a BioTek Cytation 5 plate reader (excitation 485 nm, emission 528 nm for the FBBBE dye).

1.6.3.3. GOx-SNAs activity versus native protein

20 nM native glucose oxidase protein or 20 nM GOx-SNAs were added to 1X PBS in the presence of 1 mM glucose and 5 μM FBBBE at 37 °C in triplicate. A reading of fluorescence was taken every 3 min over 2 h on a BioTek Cytation 5 (excitation 485 nm, emission 528 nm for the FBBBE dye, excitation 647 nm, emission 690 nm for the Alexa Fluor 647 dye).

1.6.3.4. Fluorescence response of GOx-SNAs in different cell lines

We tested nine different cells lines (MDA-MB-231, MC38, U87, SKOV3, HDF, EL4, EG7-OVA, 4T1, and NIH/3T3), representing a mix of cancer and normal cells, adherent and suspension cells, and human and murine-derived cells. Adherent cells were detached from culture dish using 1X TrypLE and subsequently pelleted by centrifugation. The supernatant was removed and the cells were washed twice with 6 mL glucose-free DMEM (Thermo-Fisher 11966025) through successive pelleting and resuspension steps. After the second wash, the cell suspension was split into 3

different treatment groups, each run in triplicate. In two of the treatment groups, the cells were suspended in glucose-free media only and in the third treatment group the cells were suspended in glucose-free media containing 40 nM GOx-SNAs (by protein). After 30 min at 37 °C, cells were pelleted by centrifugation, the supernatant was removed, and all cells were washed twice with 1 mL glucose-free media through successive pelleting and resuspension steps. In the first treatment group, previously untreated cells were resuspended in DMEM supplemented with 25 mM glucose (untreated group). In the second treatment group, previously untreated cells were resuspended in DMEM supplemented with 25 mM glucose and 50 µM FBBBE (dye only group). In the third treatment group, previously SNA treated cells were resuspended in DMEM supplemented with 25 mM glucose and 50 µM FBBBE (dye+SNA group). After 30 min at 37 °C, cells were pelleted by centrifugation, resuspended in 1X TrypLE containing DAPI, and analyzed using flow cytometry. This procedure was the same for all adherent cell lines.

Suspension cells were pelleted by centrifugation and washed twice with 6 mL glucose-free DMEM through successive pelleting and resuspension steps. After the second wash, the cell suspension was split into 3 different treatment groups each run in triplicate. In two of the treatment groups, cells were suspended in glucose-free media only and in the third treatment group the cells were suspended in glucose-free media containing 40 nM GOx-ProSNA (by protein). After 30 min at 37 °C, cells were pelleted by centrifugation, the supernatant was removed, and all cells were washed twice with 1 mL glucose-free media through successive pelleting and resuspension steps. In the first treatment group, previously untreated cells were resuspended in DMEM supplemented with 25 mM glucose (untreated group). In the second treatment group, previously untreated cells were resuspended in DMEM supplemented with 25 mM glucose and 50 µM FBBBE (dye only group). In the third treatment group, previously SNA treated cells were resuspended in DMEM supplemented with 25 mM glucose and 50 µM FBBBE (dye+SNA group). After 30 min at 37 °C, cells were pelleted by centrifugation, resuspended in 1X TrypLE containing DAPI, and analyzed using flow cytometry. This procedure was the same for all suspension cell lines.

1.6.3.5. Fluorescence response of GOx-SNAs in cells exposed to varying glucose concentrations

EL4 suspension cells were pelleted by centrifugation and washed twice with 6 mL glucose-free DMEM through successive pelleting and resuspension steps. After the second wash, the cell

suspension was split into different treatment groups, each run in triplicate. The cells were suspended in glucose-free media containing 40 nM GOx-SNAs (by protein). After 30 min at 37 °C, cells were pelleted by centrifugation, the supernatant was removed, and all cells were washed twice with 1 mL glucose-free media through successive pelleting and resuspension steps. The cells were then resuspended in DMEM containing 50 μM FBBBE with 0 or 25 mM glucose. After 30 min at 37 °C, cells were pelleted by centrifugation, resuspended in TrypLE containing DAPI, and analyzed using flow cytometry. Relative glucose levels in cells measured by flow cytometry were compared with glucose levels measured in cell lysates using a commercially available glucose assay kit (**Section 1.6.3.8**).

1.6.3.6. Fluorescence response of GOx-SNAs in cells when glucose uptake increases

The insulin-sensitive MC38 cell line was used in this study. MC38 cells were detached from culture dish using 1X TrypLE and subsequently pelleted by centrifugation. The supernatant was removed and the cells were washed twice with 6 mL glucose-free DMEM (Thermo-Fisher #11966025) through successive pelleting and resuspension steps. After the second wash, the cell suspension was split into different treatment groups, each run in triplicate. The cells were suspended in glucose-free media containing 40 nM GOx-SNAs (by protein). After 30 min at 37 °C, cells were pelleted by centrifugation, the supernatant was removed, and all cells were washed twice with 1 mL glucose-free media through successive pelleting and resuspension steps. The cells were resuspended in DMEM containing 5 mM glucose and 50 μM FBBBE with 0 or 100 nM insulin from Thermo Fisher catalog #12585014. After 30 min at 37 °C, cells were pelleted by centrifugation, resuspended in TrypLE containing DAPI, and analyzed using flow cytometry.

1.6.3.7. Fluorescence response of GOx-SNAs in cells when glucose uptake is inhibited

EL4 suspension cells were pelleted by centrifugation and washed twice with 6 mL glucose-free DMEM through successive pelleting and resuspension steps. After the second wash, the cell suspension was split into different treatment groups, each run in triplicate. The cells were suspended in glucose-free media containing 40 nM GOx-SNAs (by protein). After 30 min at 37 °C, cells were pelleted by centrifugation, the supernatant was removed, and all cells were washed twice with 1 mL glucose-free media through successive pelleting and resuspension steps. The cells were resuspended in DMEM containing 25 mM glucose and 50 μM FBBBE with 0 or 10 μM cytochalasin B from Millipore Sigma catalog #C6762. After 30 min at 37 °C, cells were pelleted

by centrifugation, resuspended in TrypLE containing DAPI, and analyzed using flow cytometry. Relative glucose levels in cells measured by flow cytometry were compared with glucose levels measured in cell lysates using a commercially available glucose assay kit (**Section 1.6.3.8**).

1.6.3.8. Measurement of glucose in cell lysate

EL4 cells were pelleted by centrifugation and washed twice with 6 mL glucose-free DMEM through successive pelleting and resuspension steps. After the second wash, the cell suspension was split into 3 different treatment groups, each run in triplicate. In all of the treatment groups, cells were first suspended in glucose-free media. After 30 min at 37 °C, cells were pelleted by centrifugation, the supernatant was removed, and then cells were treated in 3 groups. In the first treatment group, cells were resuspended in DMEM containing no glucose (0 mM glucose treatment group). In the second treatment group, cells were resuspended in DMEM supplemented with 25 mM glucose and 10 µM cytochalasin B (glucose inhibitor group). In the third treatment group, cells were resuspended in DMEM supplemented with 25 mM glucose (25 mM glucose treatment group). After 30 min at 37 °C, cells were combined and pelleted by centrifugation, the supernatant was removed, and cells were washed twice with 6 mL DPBS through successive pelleting and resuspension steps. After the 2nd wash, cells were resuspended in 1 mL of glucose assay buffer (Abcam 169559). Cells were then lysed through 5 freeze-thaw cycles.

After lysis, cells were centrifuged to remove any cellular debris and the supernatant was collected for further analysis. A glucose assay kit (Abcam 169559) was used to measure relative glucose concentrations between the 3 different conditions (150,000 cells analyzed in each well). Lysate was first filtered through a 10 kDa Amicon filter to remove any interfering proteins, and then assayed according to the manufacturer protocol using a BioTek Cytation 5 fluorescence plate reader.

1.7. Data analysis and statistics

All figures provided show the mean of three independent readings unless otherwise mentioned. Error bars correspond to one standard deviation. For main text Figure 2B, the p-value was determined via a t-test using a one-tailed hypothesis (this is because fluorescence at pH 5.5 should be higher than fluorescence at pH 7.5).

2. Additional results and discussion

2.1. i-motif and control gold NFs

2.1.1. Fluorescence melt to determine the melting temperature of flare strands

For a fair comparison of the false-positive signal obtained from gold NFs, it is important to ascertain that the flares strands bind to the recognition sequences with similar affinity. As a proxy for the binding affinity, we investigated the melting behavior of the duplexes. When the flare strand is hybridized to the recognition sequence, its proximity to the gold nanoparticle quenches its fluorescence. However, as the temperature of the sample is gradually increased, DNA dehybridization occurs. Therefore, the fluorescence of the flare sequence gradually increases as it is separated from the gold nanoparticle. From the figure below (Figure S5), we observe that the melting temperatures of the flare strands are nearly identical for both the i-motif and control gold NFs.

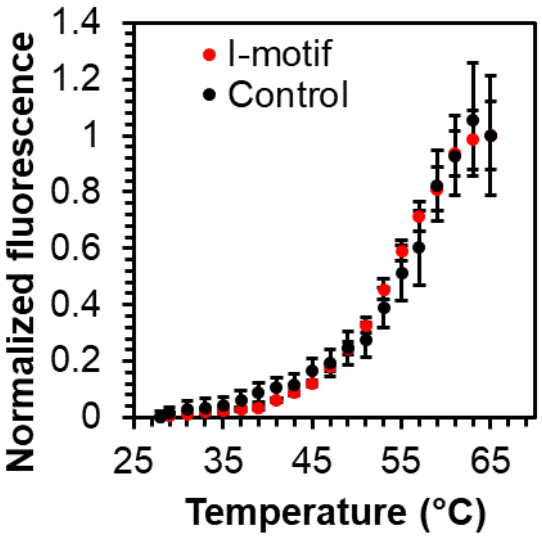

Figure S5. Fluorescence melt experiment to determine the melting temperature of pH-sensitive i-motif and pH-insensitive control NFs recognition/flare duplex. It can be seen from the plot that the melting temperatures are nearly identical. Data points and error bars represent the mean and standard deviation of three replicates, respectively.

2.1.2. pH-sensitivity of i-motif gold NFs in buffer

~1.7 nM of i-motif and control gold NFs were subjected to different pH between 7.5 and 4.5 at 37 °C and their fluorescence was monitored. The fluorescence of i-motif gold NFs increases by up to ~3.5-fold as the pH decreases due to the formation of i-motif structures and displacement of the flare sequence. In contrast, the fluorescence of the pH-insensitive control NF does not change significantly in this pH range.

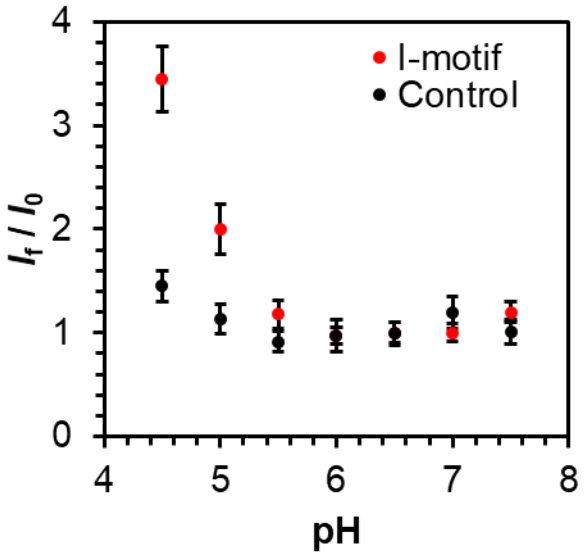

Figure S6. Fluorescence enhancement (I_f / I_0) versus pH for gold NF constructs in buffer. Fluorescence enhancement is defined as the fluorescence intensity of the solution at a given pH (I_f) relative to the lowest fluorescence intensity of the solution across all the pH tested (I_0). All fluorescence intensities are corrected for the fluorescence intensity of the buffer. Data points and error bars represent the mean and standard deviation of three replicates, respectively.

2.1.3. Fluorescence response of gold NFs in the presence of nucleases in buffer

To investigate the effect of nuclease degradation on gold NFs, 2 nM gold NFs were incubated with 2 U DNAse I for at 37 °C. In the presence of DNAse I, the fluorescence increases over time for both the i-motif and the control sequence. In contrast, in the absence of DNAse I, the fluorescence remains unchanged. These results show that nuclease degradation leads to over 15-fold fluorescence enhancement in the absence of a recognition event, giving rise to false-positive signals.

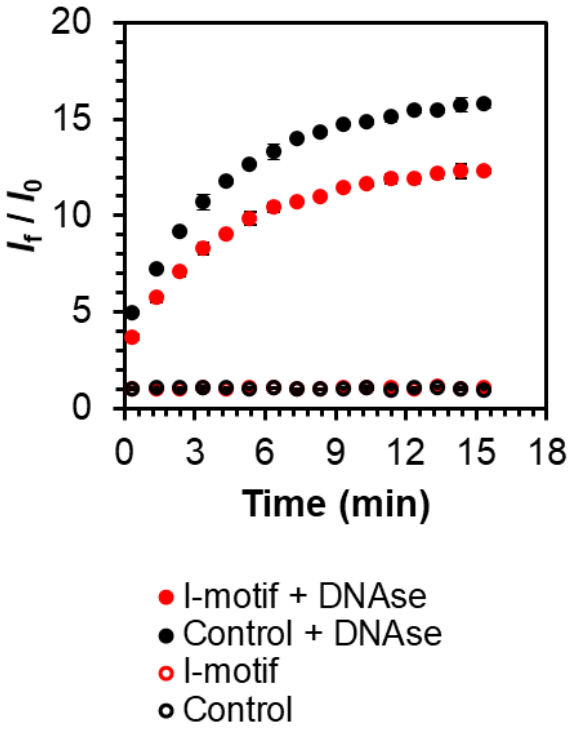

Figure S7. Fluorescence enhancement over time of 100 µL of 2 nM i-motif or control gold NF in the presence of 10 µL of 0.2 U/µL DNAse I. Fluorescence enhancement is defined as the fluorescence intensity of the solution at a given time (I_f) relative to the initial fluorescence intensity of the same solution (I_0). All fluorescence intensities are corrected for the fluorescence intensity of the buffer. In the presence of DNAse I, the fluorescence increases by over 15-fold while in the absence of DNAse I, the fluorescence remains unchanged. Data points and error bars represent the mean and standard deviation of three replicates, respectively.

2.1.4. Change in fluorescence signal over time of control gold NFs *in cellulo*

To determine the extent of false-positive signal obtained from NFs in cells, pulse-chase experiments were performed with the control gold NFs. 1 nM of the control NFs were incubated with MDA-MB-231 cells for 1 h in serum-free media. The cells were then washed thoroughly and after additional 0, 2, and 4 h, they were analyzed by flow cytometry. The fluorescence from the flare strand was monitored and found to increase over time. These results show that a time-dependent false-positive fluorescence signal is observed from gold NFs in cells.

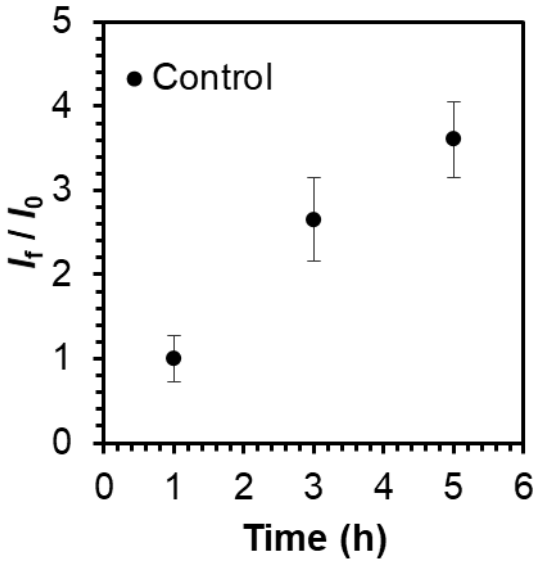

Figure S8. Fluorescence enhancement over time of MDA-MB-231 cells treated with control gold NFs. Fluorescence enhancement is defined as the mean fluorescence intensity of the cells at a given time (I_f) relative to the mean fluorescence intensity (I_0) at the initial timepoint. All fluorescence intensities are corrected for the mean fluorescence intensity of untreated cells. Time 1 h corresponds to a 1 h pulse, 0 h chase. Time 3 h corresponds to a 1 h pulse, 2 h chase. Time 5 h corresponds to 1 h pulse, 4 h chase. The fluorescence increases by ~3.5 fold over time. Data points and error bars represent the mean and standard deviation of three replicates, respectively.

2.2. ProTOn and control ProSNAs

2.2.1. Fluorescence response of ProSNAs in presence of nuclease in buffer

To investigate the effect of nuclease degradation on ProSNAs, 500 nM (by DNA) of ProTOn or control ProSNA were incubated with 2 U DNAse I for at 37 °C. The fluorescence remains unchanged in both the presence and absence of DNAse I. These results show that nuclease degradation does not give rise to a false-positive signal.

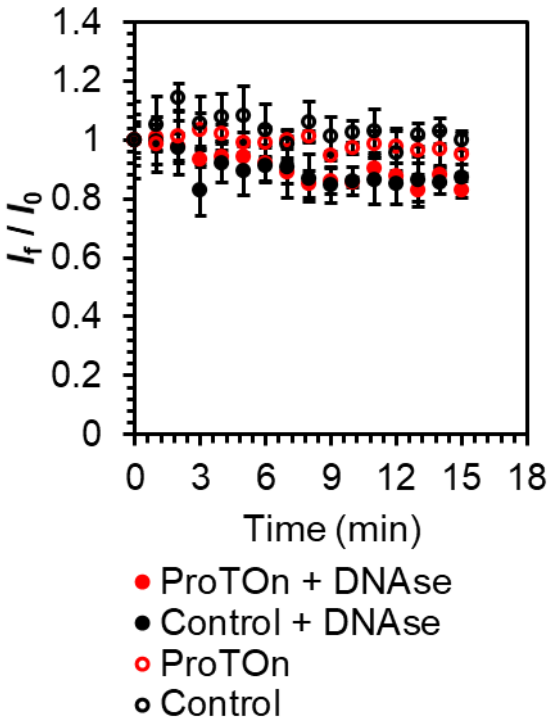

Figure S9. Fluorescence enhancement over time of 100 µL of 500 nM (by DNA) of ProTOn or control ProSNA in the presence of 10 µL of 0.2 U/µL DNAse I. The fluorescence of samples without DNAse I was monitored over time as a control. Fluorescence enhancement is defined as the fluorescence intensity at a given time (I_f) relative to the fluorescence intensity (I_0) at the initial timepoint. All fluorescence intensities are corrected for the fluorescence intensity of the buffer. Data points and error bars represent the mean and standard deviation of three replicates, respectively.

2.2.2. Change in fluorescence signal over time of control ProSNAs *in cellulo*

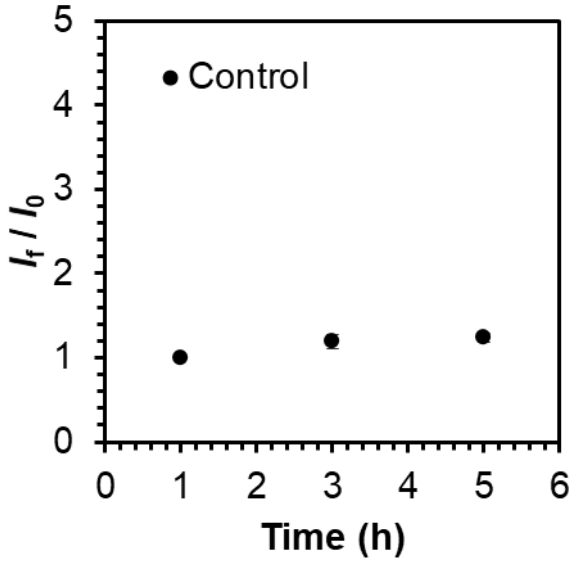

Figure S10. Fluorescence enhancement over time of MDA-MB-231 cells treated with control ProSNAs. Fluorescence enhancement is defined as the mean fluorescence intensity of the cells at a given time (I_f) relative to the mean fluorescence intensity (I_0) at the initial timepoint. All fluorescence intensities are corrected for the mean fluorescence intensity of untreated cells. Time 1 h corresponds to a 1 h pulse, 0 h chase. Time 3 h corresponds to a 1 h pulse, 2 h chase. Time 5 h corresponds to a 1 h pulse, 4 h chase. Unlike with gold NFs (**Figure S8**), the fluorescence does not significantly change over time. Data points and error bars represent the mean and standard deviation of three replicates, respectively.

2.2.3. Fluorescence response of pHrodo™ Red AM Intracellular pH Indicator

To benchmark ProTOn against a commercially available intracellular pH indicator, we studied the pH response of pHrodo™ Red AM. This hydrophobic pH-sensitive dye is cell permeable. In the cell, non-specific esterases cleave the AM ester groups and, consequently, the dye is retained intracellularly. We studied the pH response of pHrodo™ Red AM both in buffered solutions as well as in cells clamped to specific pH.

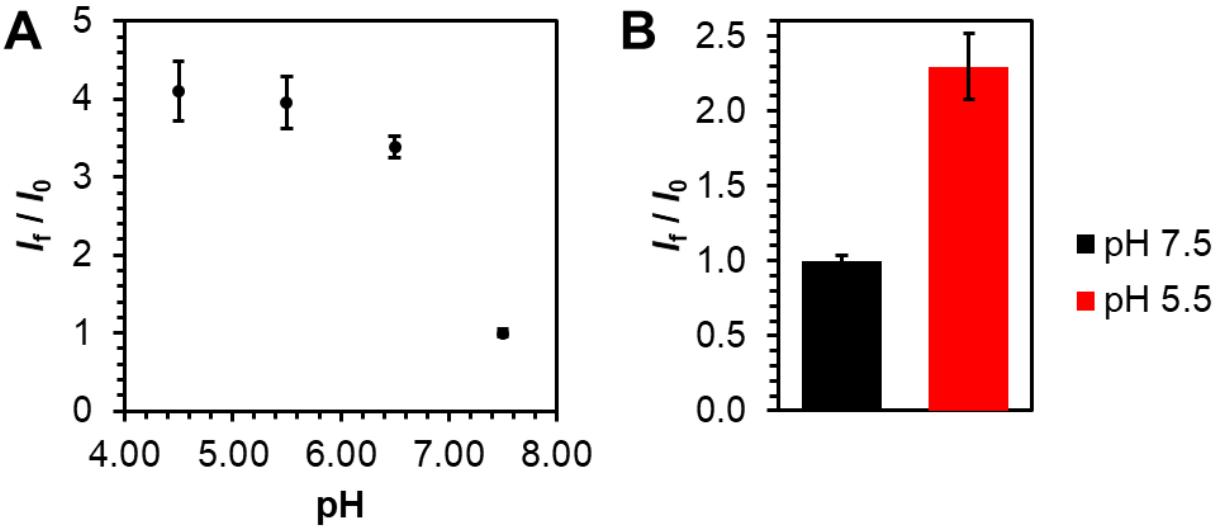

Figure S11. Fluorescence enhancement of pHrodo™ Red in (A) buffer at different pH (500 nM pHrodo, excitation: 560 nm, emission: 610 nm) and (B) cells clamped at different pH. Fluorescence enhancement is defined as the fluorescence intensity of the pHrodo™ Red solution/cells at a given pH (I_f) relative to the fluorescence intensity (I_0) at pH 7.5. All fluorescence intensities are corrected for the fluorescence intensity of the buffer/untreated cells. Intracellularly, pHrodo™ Red results in an approximately ~2-fold fluorescence enhancement when clamped at pH 5.5 relative to pH 7.5. Data points and error bars represent the mean and standard deviation of three replicates, respectively.

2.2.4. The ProSNA architecture protects the protein against protease degradation

To demonstrate the effectiveness of the SNA architecture in protecting a protein from protease degradation, both the native protein and the ProSNA were incubated with a protease (trypsin) and aliquots of this degradation reaction were loaded on an SDS-PAGE gel. We observed that the native protein incubated with trypsin produced several lower molecular weights corresponding to degradation products after 10 min. Furthermore, the intensity of these degradation products increased with time. However, with the ProSNA these degradation bands were not observed suggesting that the DNA shell is able to partially protect the protein from substantial degradation by trypsin.

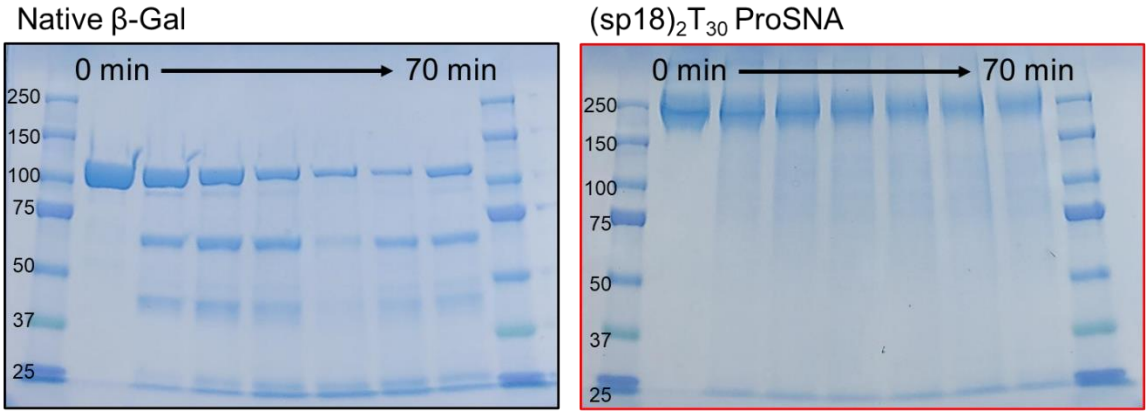

Figure S12. SDS-PAGE gel of β-gal and β-gal ProSNA treated with trypsin (protease) shows that while β-gal degrades over a time course of 70 min (as evidenced by the appearance of multiple bands at lower molecular weights), β-gal ProSNA does not. The β-gal ProSNA used in this specific study consists of the DNA sequence 5'-DBCO-dT-$(sp18)_2T_{30}$-3'.

2.3. GOx-SNAs

2.3.1. GOx-characterization

Since this is the first report of GOx-SNAs, we provide UV-vis characterization data below. We note that native GOx has an absorbance peak at 280 nm. Upon modifying the GOx with AF-647 and PEG azides (i.e. for GOx-AP), an additional absorbance peak is observed at 650 nm corresponding to AF-647. Upon further functionalization with DNA (i.e. for GOx-SNAs), an additional peak is observed at 260 nm corresponding to the DNA. Based on the extinction coefficients of the GOx, AF-647, and DNA, the number of AF-647 dyes per GOx-SNA were calculated to be ~2 while the number of DNA strands were calculated to be ~28.

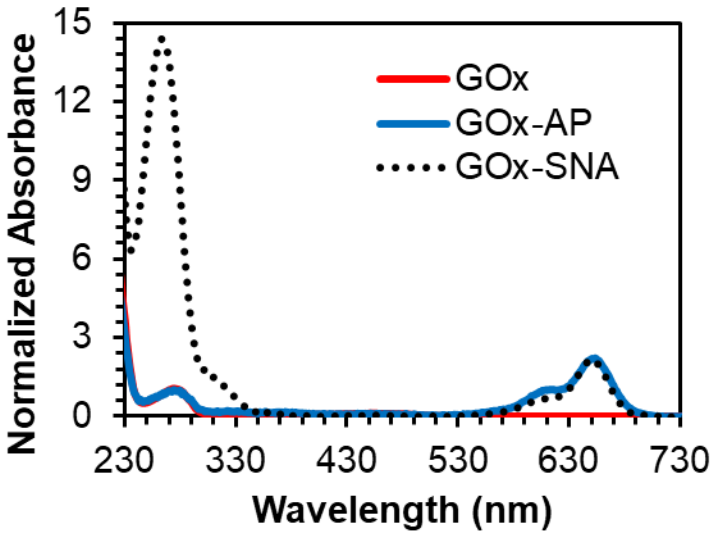

Figure S13. UV-vis characterization of GOx-SNAs. The absorbance is normalized relative to the GOx peak at 280 nm which is set to a value of 1.

2.3.2. Activity of GOx-SNAs compared to native GOx

To determine the effect of conjugation of DNA to GOx on its catalytic activity, we incubated identical concentrations (20 nM) of GOx and GOx-SNAs with and without 1 mM glucose in 1X PBS containing 5 µM FBBBE at 37 °C. GOx catalyzes the conversion of glucose to gluconic acid with concomitant production of hydrogen peroxide. The hydrogen peroxide formed reacts with FBBBE and cleaves the boronate ester groups, yielding highly fluorescent fluorescein. We observe from the figure below that the fluorescence increases significantly over time in the presence of glucose. Importantly, the increase in fluorescence for both GOx and GOx-SNAs is nearly identical showing that the activity of GOx is retained in SNA form.

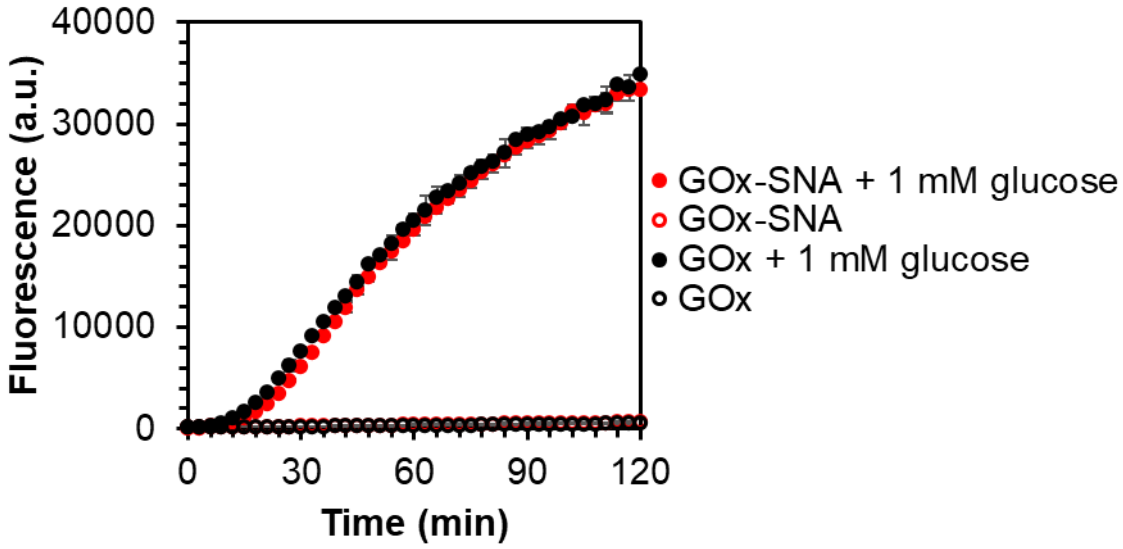

Figure S14. Comparison of catalytic activity of GOx and GOx-SNAs at 37 °C. 20 nM GOx-SNA or 20 nM native GOx are treated with 0 mM or 1 mM glucose in 1X PBS containing 5 µM FBBBE. The fluorescence at each time point is corrected for the fluorescence of the dye alone in buffer. The fluorescence is monitored by exciting FBBBE at 485 nm and collecting the emission at 528 nm. The results show that the protein's native activity is retained in the SNA form. Data points and error bars represent the mean and standard deviation of three replicates, respectively.

2.3.3. Response of GOx-SNAs to increasing glucose concentrations in buffer

To determine the response of GOx-SNAs to increasing glucose concentrations in buffer, we incubated 20 nM GOx-SNAs with 5 µM FBBBE in 1X PBS at 37 °C and added varying amounts of glucose between 0-5 mM. The fluorescence from FBBBE was monitored over a period of 2 h. A calibration curve was constructed at the 30 min and 2 h time points. The limit of detection (LOD) was determined at each time point by the $3\sigma/m$ method, where σ denotes the standard deviation of the response and m denotes the initial slope of the calibration curve. The LODs were to be ~17 µM and ~5 µM at 30 min and 2 h, respectively. Both LODs are well below the typical concentration of glucose in cells (0.1 - 2 mM).[6,7]

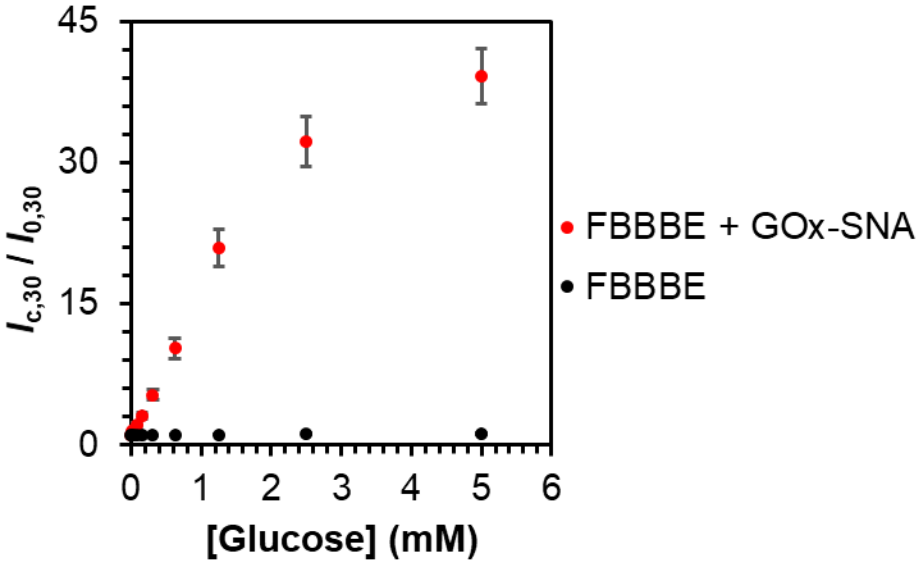

Figure S15. Fluorescence enhancement of 20 nM GOx-SNAs + 5 µM FBBBE in the presence of varying amounts of glucose at 37 °C. The fluorescence enhancement is calculated as the ratio, $I_{c,30}$ / $I_{0,30}$. $I_{c,30}$ represents the fluorescence of the solution at the 30 min time point when a concentration c of glucose is added. $I_{0,30}$ represents the fluorescence of the solution at the 30 min time point when a concentration of 0 mM of glucose is added. The fluorescence is corrected for the fluorescence of the buffer. The fluorescence is monitored by exciting FBBBE at 460 nm and collecting the emission at 530 nm. Data points and error bars represent the mean and standard deviation of three replicates, respectively.

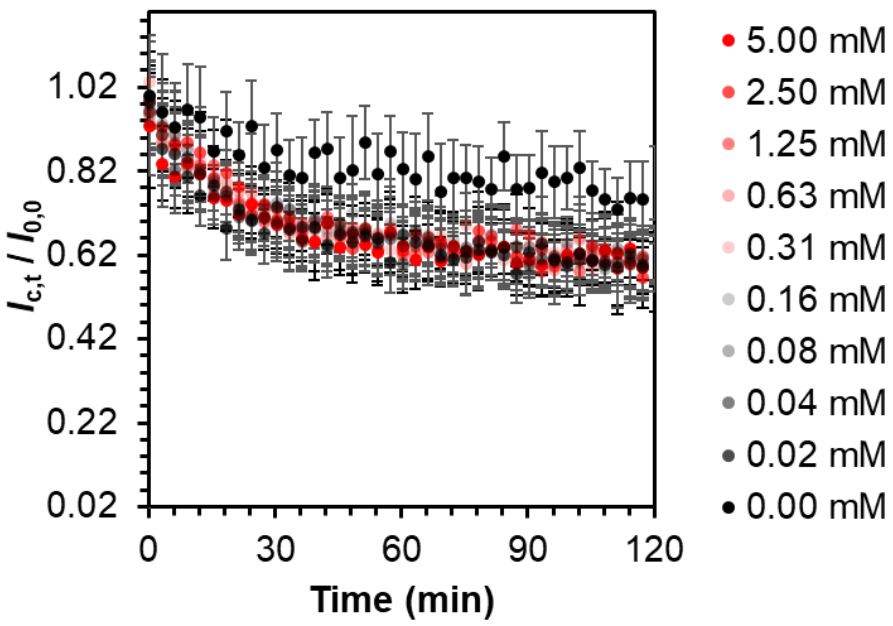

Figure S16. Fluorescence enhancement over time of AF-647 conjugated to GOx-SNAs in the presence of varying amounts of glucose and 5 µM FBBBE 1X PBS at 37 °C. The fluorescence enhancement is calculated as the ratio of $I_{c,t}$ / $I_{0,0}$. $I_{c,t}$ represents the fluorescence of the solution at the time *t* when a concentration *c* of glucose is added. $I_{0,0}$ represents the fluorescence of the solution at the initial time point when a concentration of 0 mM of glucose is added. These results show that the AF-647 signal from GOx-SNAs is not affected by the formation of FBBBE. The slight decrease in fluorescence over time is attributed to photobleaching. The fluorescence is monitored by exciting GOx-SNAs at 640 nm and collecting the emission at 700 nm. Data points and error bars represent the mean and standard deviation of three replicates, respectively.

2.3.4. Selectivity of GOx-SNAs for glucose over other sugars in a complex mixture

We studied whether GOx-SNAs can selectively detect glucose in the presence of other sugars (sucrose, xylose, mannose, fructose, maltose, lactose, galactose, and glucose-6-phosphate). We note that the fluorescence observed in the presence of glucose is nearly identical to the fluorescence observed when glucose is present in a mixture of other sugars. Importantly, the fluorescence observed in the absence of glucose is negligible.

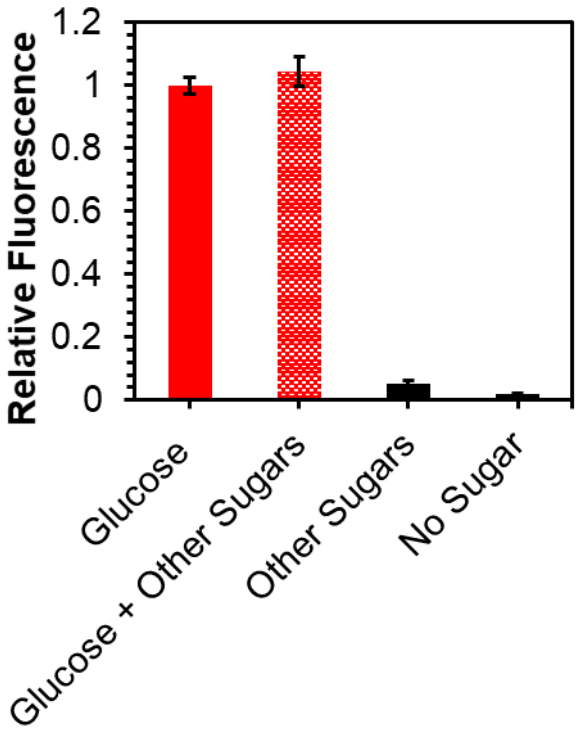

Figure S17. Selectivity of GOx-SNAs for glucose over other sugars in a complex mixture. 10 nM GOx-SNAs were incubated with 5 μM FBBBE at 37 °C for 30 min in the presence or absence of 5 mM of sugars. The fluorescence observed when 5 mM glucose is added to the GOx-SNA/FBBBE solution is normalized to a value of one. The other values are plotted relative to this value. The fluorescence of all three data points was corrected for the fluorescence of a solution of containing only FBBBE. The fluorescence was monitored by exciting FBBBE at 485 nm and collecting the emission at 528 nm. Data points and error bars represent the mean and standard deviation of three replicates, respectively.

2.3.5. Response of GOx-SNAs in different cell lines

2.3.5.1. Example flow cytometry gating strategy

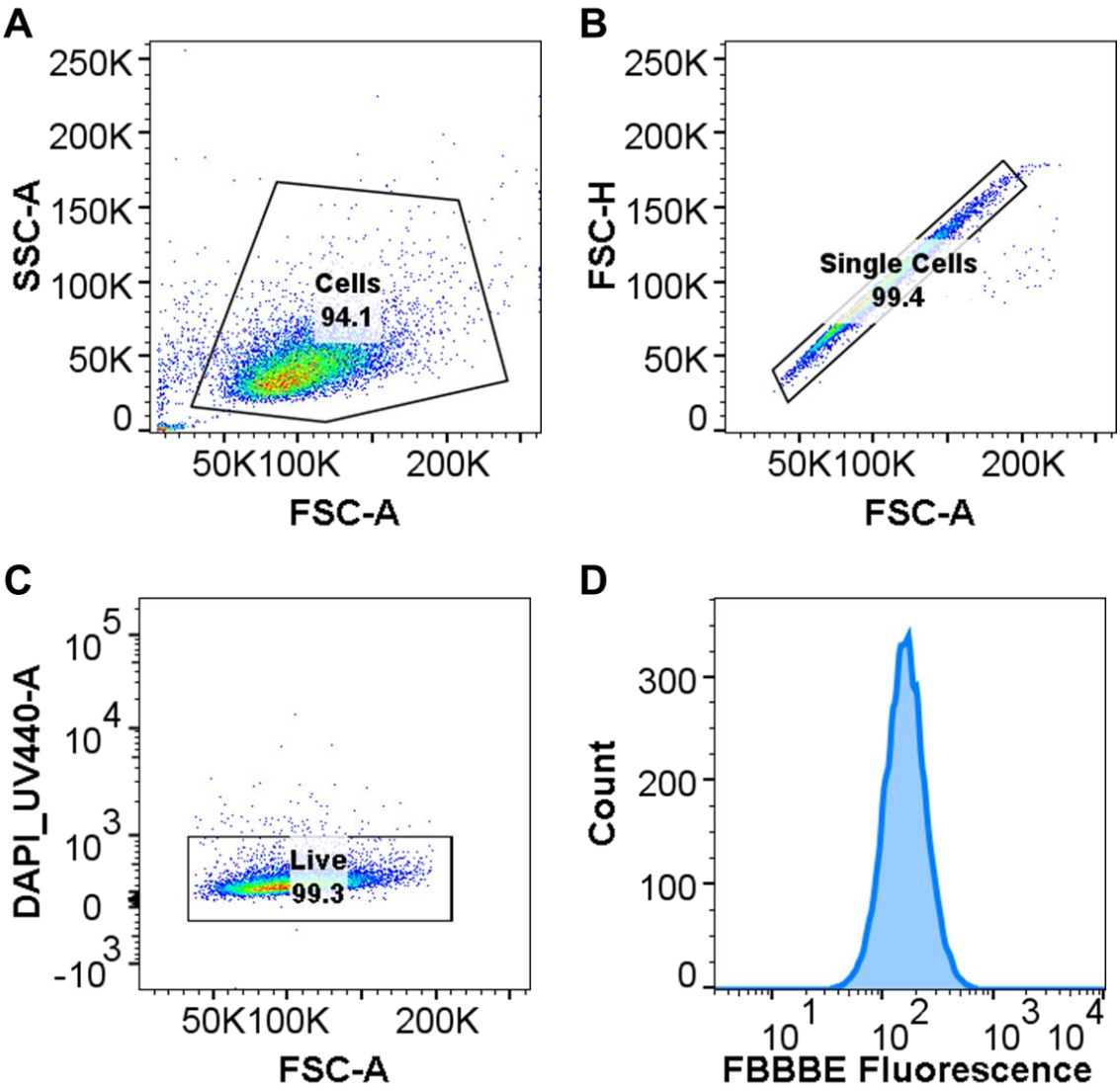

Figure S18. Example flow cytometry gating strategy. (A) Cells are first distinguished from debris based on forward and side scatter. (B) Single cells are distinguished from clusters of cells. (C) Live cells are selected based on the fluorescence of the dye DAPI which preferentially stains dead cells. (D) The fluorescence histogram of live cells in the FBBBE channel is plotted. In this example, EG7-OVA cells treated with FBBBE were analyzed.

2.3.5.2. MDA-MB-231

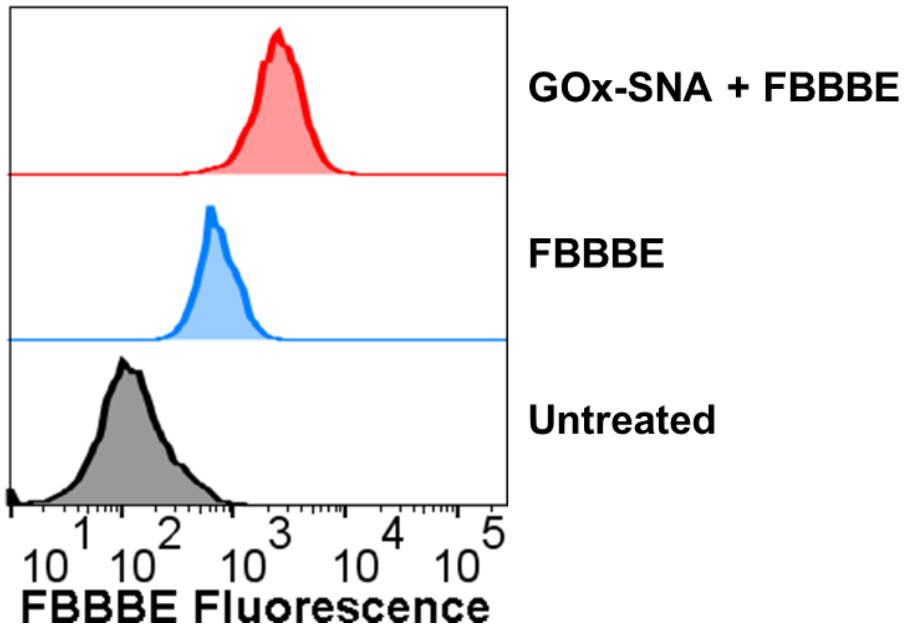

Figure S19. Glucose detection in MDA-MB-231 cells. Representative fluorescence histograms of untreated cells, cells treated with 50 µM FBBBE, and cells treated with 40 nM GOx-SNA and 50 µM FBBBE.

2.3.5.3. U87

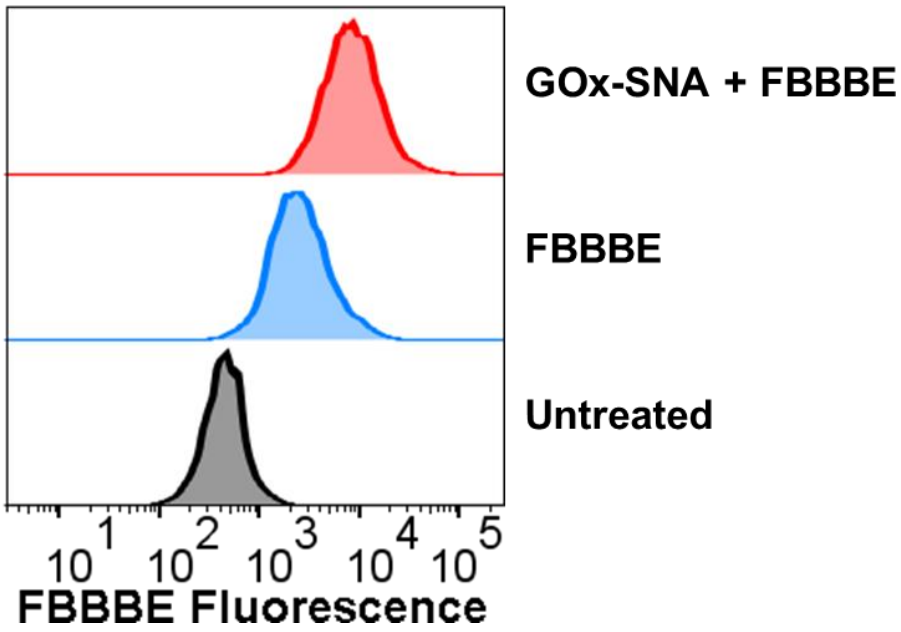

Figure S20. Glucose detection in U87 cells. Representative fluorescence histograms of untreated cells, cells treated with 50 µM FBBBE, and cells treated with 40 nM GOx-SNA and 50 µM FBBBE.

2.3.5.4. SKOV-3

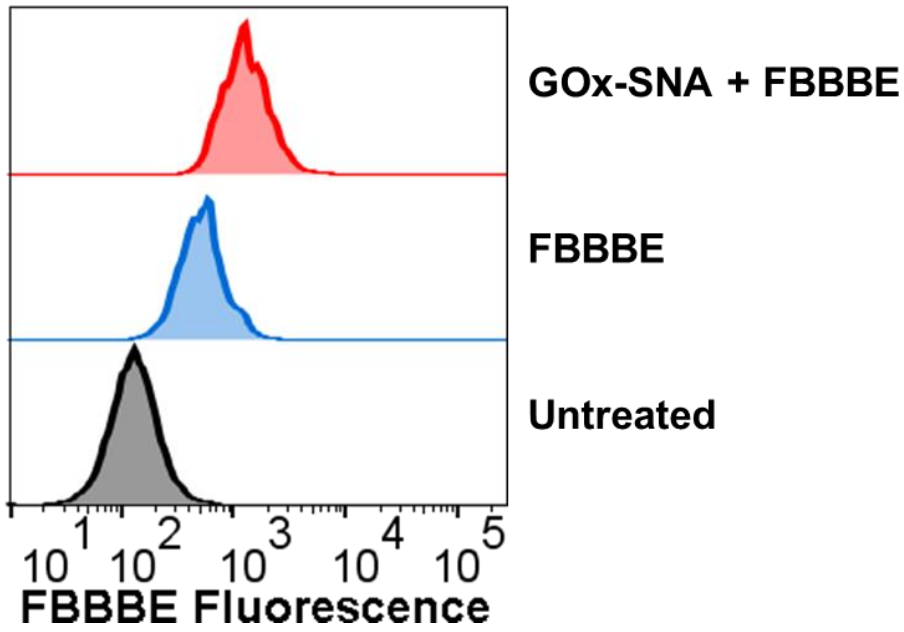

Figure S21. Glucose detection in SKOV-3 cells. Representative fluorescence histograms of untreated cells, cells treated with 50 µM FBBBE, and cells treated with 40 nM GOx-SNA and 50 µM FBBBE.

2.3.5.5. EL4

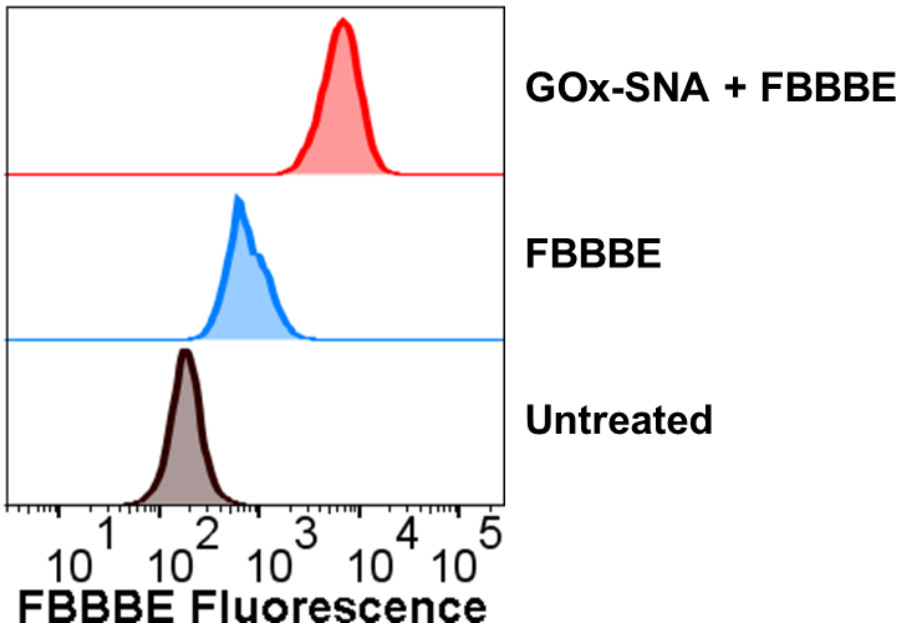

Figure S22. Glucose detection in EL4 cells. Representative fluorescence histograms of untreated cells, cells treated with 50 µM FBBBE, and cells treated with 40 nM GOx-SNA and 50 µM FBBBE.

2.3.5.6. Human Dermal Fibroblasts (HDF)

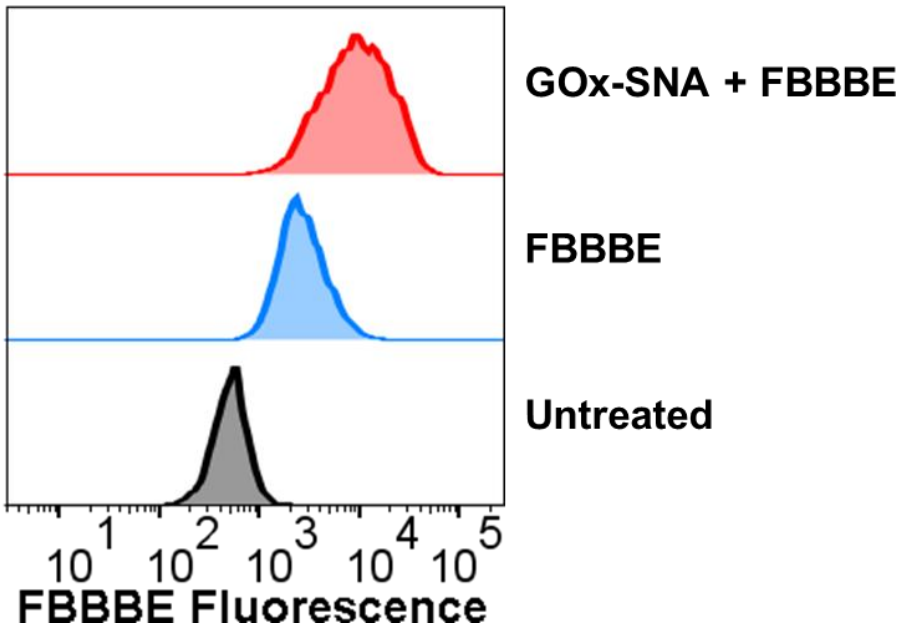

Figure S23. Glucose detection in HDF cells. Representative fluorescence histograms of untreated cells, cells treated with 50 µM FBBBE, and cells treated with 40 nM GOx-SNA and 50 µM FBBBE.

2.3.5.7. MC38

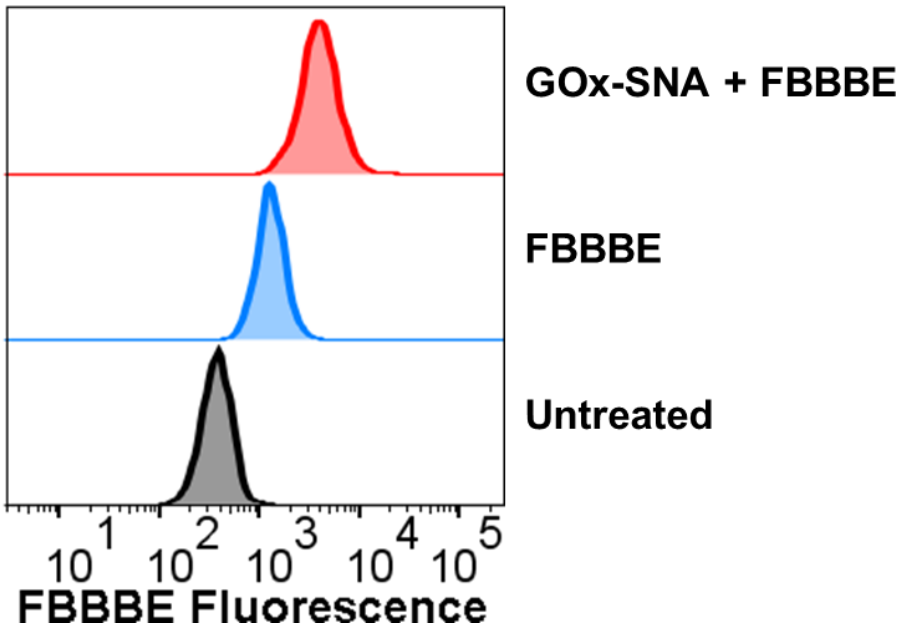

Figure S24. Glucose detection in MC38 cells. Representative fluorescence histograms of untreated cells, cells treated with 50 µM FBBBE, and cells treated with 40 nM GOx-SNA and 50 µM FBBBE.

2.3.5.8. NIH-3T3

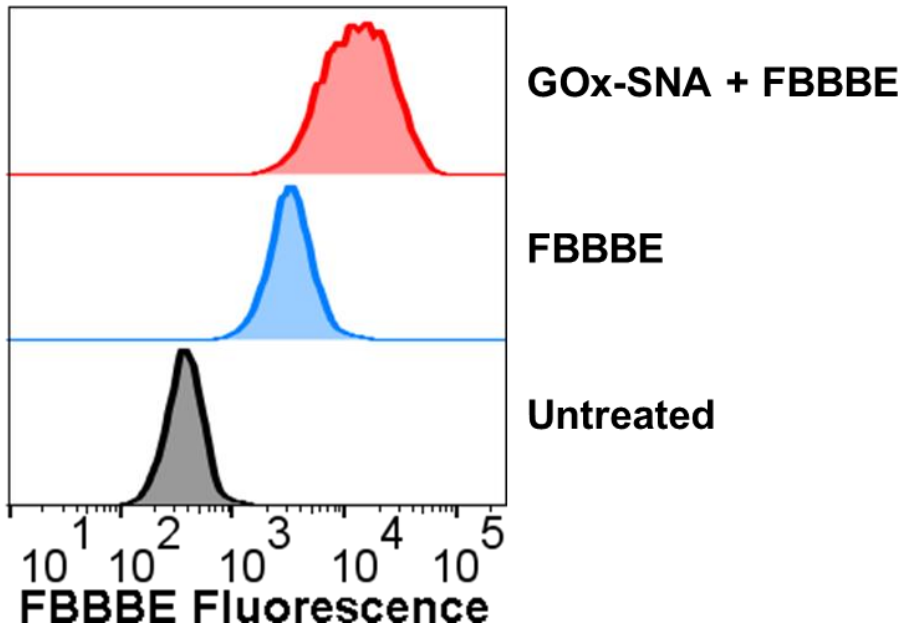

Figure S25. Glucose detection in NIH-3T3 cells. Representative fluorescence histograms of untreated cells, cells treated with 50 µM FBBBE, and cells treated with 40 nM GOx-SNA and 50 µM FBBBE.

2.3.5.9. 4T1

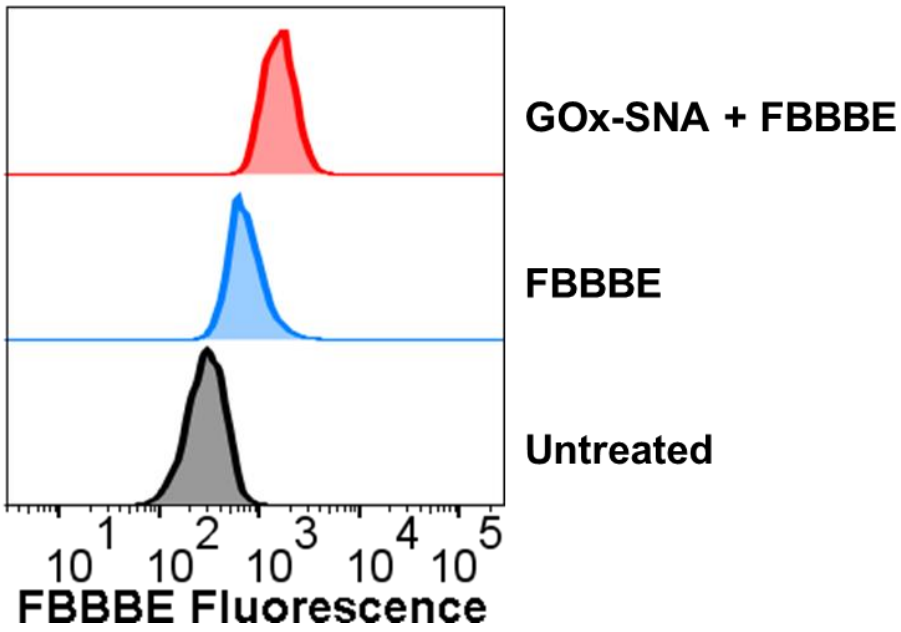

Figure S26. Glucose detection in 4T1 cells. Representative fluorescence histograms of untreated cells, cells treated with 50 µM FBBBE, and cells treated with 40 nM GOx-SNA and 50 µM FBBBE.

2.3.5.10. EG7-OVA

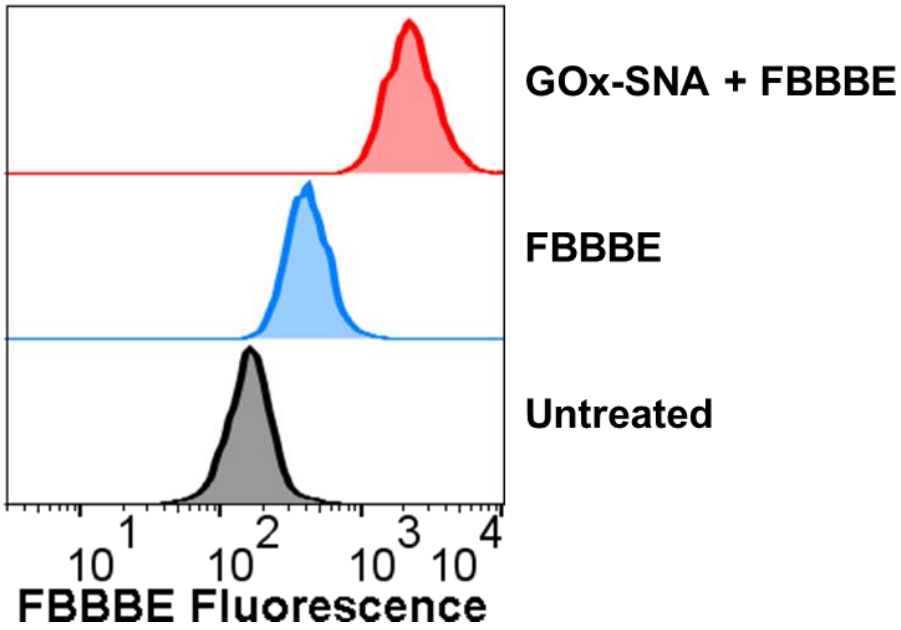

Figure S27**.** Glucose detection in EG7-OVA cells. Representative fluorescence histograms of untreated cells, cells treated with 50 µM FBBBE, and cells treated with 40 nM GOx-SNA and 50 µM FBBBE.

2.3.6. Intracellular response of GOx-SNAs to varying glucose concentrations in cell culture media

To study the effect of glucose added to cell culture media on the fluorescence reported by GOx-SNAs, EL4 cells were first treated with 40 nM GOx-SNAs in glucose-free media. After washing the cells thoroughly, 50 μM FBBBE in 0 or 25 mM glucose-containing media was added to the cells. The cells were incubated at 37 °C for 30 min and then analyzed by flow cytometry. We note that the fluorescence of cells subjected to 25 mM glucose-containing media is ~50% higher than cells incubated in 0 mM glucose. Importantly, these results agree with the fluorescence observed from cell lysates when a commercially available glucose assay kit is used.

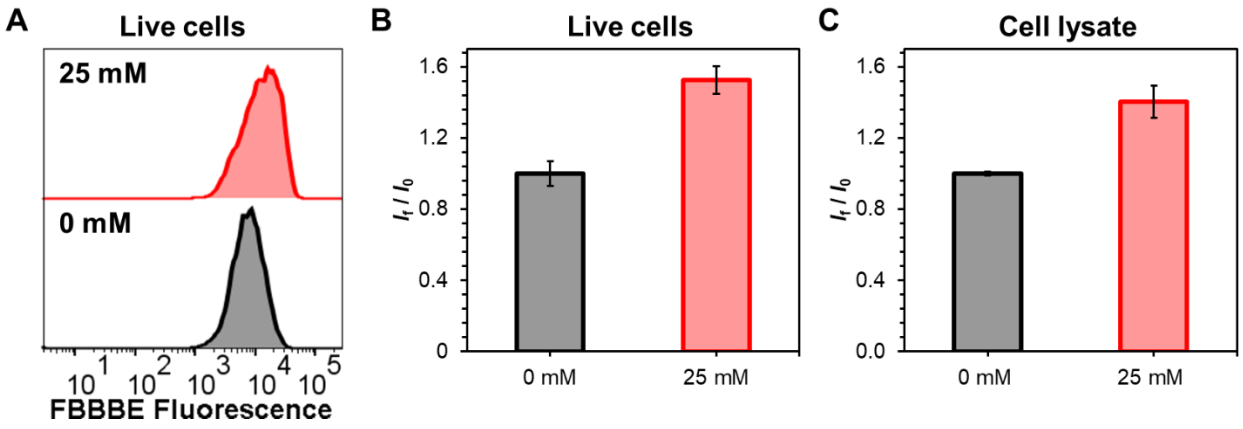

Figure S28. Intracellular response of GOx-SNAs to varying glucose concentrations in cell culture media. (A) Representative fluorescence histograms of GOx-SNA-treated cells incubated in cell culture media containing 0 and 25 mM glucose. (B) Mean fluorescence of GOx-SNA-treated cells incubated in cell culture media containing different glucose concentrations (I_f) relative to the mean fluorescence of cells incubated in 0 mM glucose-containing media (I_0). Data points and error bars represent the mean and standard deviation of three replicates, respectively. (C) Relative fluorescence values of cells incubated in cell culture media containing 0 and 25 mM glucose as measured using cell lysates through a commercially available glucose assay kit. Data points and error bars represent the mean and standard deviation of three replicates, respectively.

2.3.7. Intracellular response of GOx-SNAs to increased glucose uptake

To study the effect of increased glucose uptake on the fluorescence reported by GOx-SNAs, MC38 cells were first treated with 40 nM GOx-SNAs in glucose-free media. After washing the cells thoroughly, 50 μM FBBBE in 5 mM glucose-containing media was added to the cells. Additionally, either 0 or 100 nM insulin, well-known to increase glucose uptake, was added.[8,9] The cells were incubated at 37 °C for 30 min and then analyzed by flow cytometry. We note that the fluorescence of cells subjected to 100 nM insulin is increased by ~90% compared to cells not treated with the insulin. Importantly, these results agree with previous reports of the effect of insulin on glucose uptake in MC38 cells measured using radiolabeled glucose.[8]

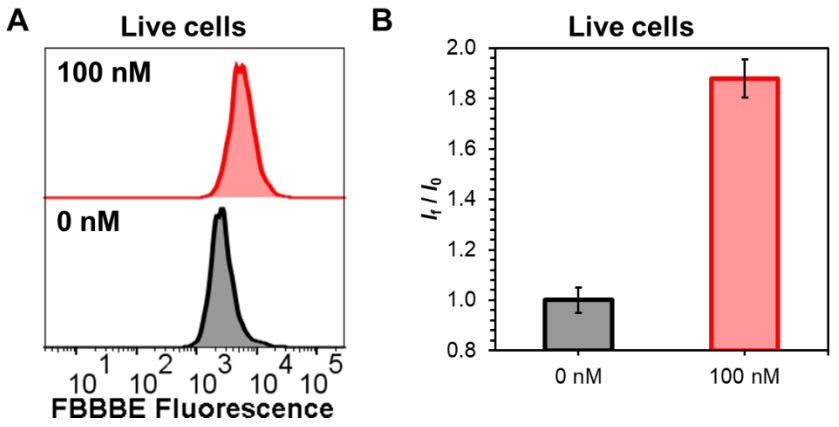

Figure S29. Intracellular response of GOx-SNAs to increase of glucose uptake. (A) Representative fluorescence histograms of GOx-SNA-treated cells incubated in cell culture media containing 0 and 100 nM insulin. (B) Mean fluorescence of GOx-SNA-treated cells incubated in cell culture media containing different insulin concentrations (I_f) relative to the mean fluorescence of cells incubated in 0 nM insulin-containing media (I_0). Data points and error bars represent the mean and standard deviation of two replicates, respectively.

2.3.8. Intracellular response of GOx-SNAs to inhibition of glucose uptake

To study the effect of blocking glucose receptors on the fluorescence reported by GOx-SNAs, EL4 cells were first treated with 40 nM GOx-SNAs in glucose-free media. After washing the cells thoroughly, 50 μM FBBBE in 25 mM glucose-containing media was added to the cells. Additionally, either 0 or 10 μM cytochalasin B, a well-known glucose transport inhibitor, was added.[10] The cells were incubated at 37 °C for 30 min and then analyzed by flow cytometry. We note that the fluorescence of cells subjected to 10 μM cytochalasin B is reduced by ~25% compared to cells not treated with the inhibitor. Importantly, these results agree with the fluorescence observed from cell lysates when a commercially available glucose assay kit is used.

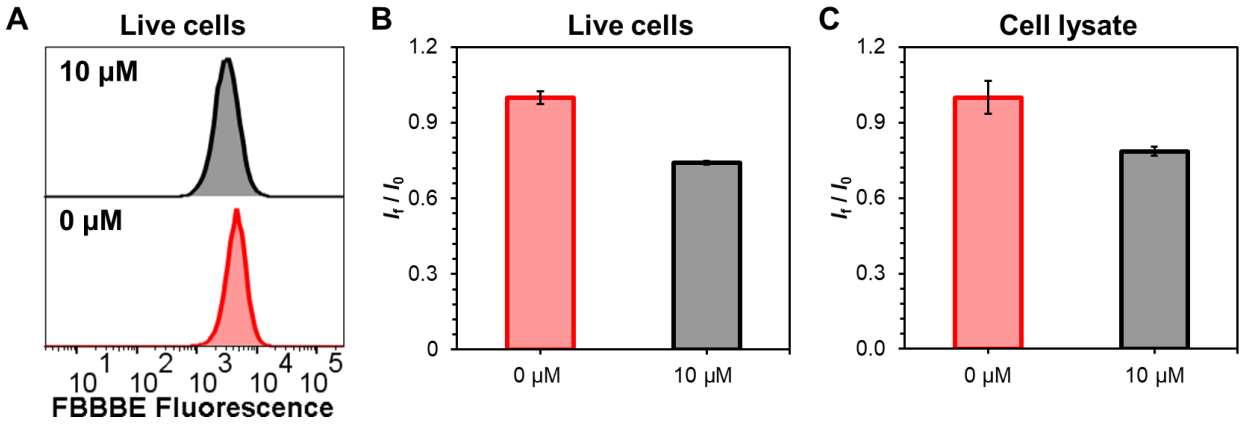

Figure S30. Intracellular response of GOx-SNAs to inhibition of glucose uptake. (A) Representative fluorescence histograms of GOx-SNA-treated cells incubated in cell culture media containing 0 and 10 μM cytochalasin B. (B) Mean fluorescence of GOx-SNA-treated cells incubated in cell culture media containing different cytochalasin B concentrations (I_f) relative to the mean fluorescence of cells incubated in 0 μM cytochalasin B-containing media (I_0). Data points and error bars represent the mean and standard deviation of three replicates, respectively. (C) Relative fluorescence values of cells incubated in cell culture media containing 0 and 10 μM cytochalasin B as measured using cell lysates through a commercially available glucose assay kit. Data points and error bars represent the mean and standard deviation of three replicates, respectively.

3. References

(1) Bethge, L.; Jarikote, D. V.; Seitz, O. New Cyanine Dyes as Base Surrogates in PNA: Forced Intercalation Probes (FIT-Probes) for Homogeneous SNP Detection. *Bioorg. Med. Chem.* **2008**, *16* (1), 114–125.

(2) Ebrahimi, S. B.; Samanta, D.; Cheng, H. F.; Nathan, L. I.; Mirkin, C. A. Forced Intercalation (FIT)-Aptamers. *J. Am. Chem. Soc.* **2019**, *141* (35), 13744–13748.

(3) Halo, T. L.; McMahon, K. M.; Angeloni, N. L.; Xu, Y.; Wang, W.; Chinen, A. B.; Malin, D.; Strekalova, E.; Cryns, V. L.; Cheng, C.; Mirkin, C. A.; Thaxton, C. S. NanoFlares for the Detection, Isolation, and Culture of Live Tumor Cells from Human Blood. *Proc. Natl. Acad. Sci. U. S. A.* **2014**, *111* (48), 17104–17109.

(4) Kusmierz, C. D.; Bujold, K. E.; Callmann, C. E.; Mirkin, C. A. Defining the Design Parameters for in Vivo Enzyme Delivery Through Protein Spherical Nucleic Acids. *ACS Cent. Sci.* **2020**, *6* (5), 815–822.

(5) Brodin, J. D.; Sprangers, A. J.; McMillan, J. R.; Mirkin, C. A. DNA-Mediated Cellular Delivery of Functional Enzymes. *J. Am. Chem. Soc.* **2015**, *137* (47), 14838–14841.

(6) Nascimento, R. A. S.; Özel, R. E.; Mak, W. H.; Mulato, M.; Singaram, B.; Pourmand, N. Single Cell "Glucose Nanosensor" Verifies Elevated Glucose Levels in Individual Cancer Cells. *Nano Lett.* **2016**, *16* (2), 1194–1200.

(7) Cline, G. W.; Petersen, K. F.; Krssak, M.; Shen, J.; Hundal, R. S.; Trajanoski, Z.; Inzucchi, S.; Dresner, A.; Rothman, D. L.; Shulman, G. I. Impaired Glucose Transport as a Cause of Decreased Insulin-Stimulated Muscle Glycogen Synthesis in Type 2 Diabetes. *N. Engl. J. Med.* **1999**, *341* (4), 240–246.

(8) Rabin-Court, A.; Rodrigues, M. R.; Zhang, X.-M.; Perry, R. J. Obesity-Associated, but Not Obesity-Independent, Tumors Respond to Insulin by Increasing Mitochondrial Glucose Oxidation. *PLoS One* **2019**, *14* (6), e0218126.

(9) Leto, D.; Saltiel, A. R. Regulation of Glucose Transport by Insulin: Traffic Control of GLUT4. *Nat. Rev. Mol. Cell Biol.* **2012**, *13* (6), 383–396.

(10) Estensen, R. D.; Plagemann, P. G. W. Cytochalasin B: Inhibition of Glucose and Glucosamine Transport. *Proc. Natl. Acad. Sci.* **1972**, *69* (6), 1430–1434.